Saccadic suppression by way of retinal-circuit image processing

Saad Idrees[1,†], Matthias-Philipp Baumann[1,2,†], Felix Franke[3], Thomas A. Münch[1,4,*], Ziad M. Hafed[1,2,*]

[1] Werner Reichardt Centre for Integrative Neuroscience, University of Tübingen, Tübingen, Germany.

[2] Hertie Institute for Clinical Brain Research, University of Tübingen, Tübingen, Germany.

[3] Bio Engineering Laboratory, ETH Zürich, Basel, Switzerland.

[4] Institute for Ophthalmic Research, University of Tübingen, Germany

* Correspondence to: ziad.m.hafed@cin.uni-tuebingen.de and thomas.muench@cin.uni-tuebingen.de

[†] Contributed equally

Abstract

Visual sensitivity is strongly impaired around the time of rapid eye movements. This robust perceptual phenomenon, called saccadic suppression, is frequently attributed to active suppressive signals that are directly derived from eye movement commands. Here, we show instead that visual-only mechanisms, activated by retinal-image shifts, can account for all perceptual properties of saccadic suppression that we have investigated. Such mechanisms start at the very first stage of visual processing in the brain, the retina. Critically, suppression originating in the retina outlasts perceptual suppression around the time of saccades, suggesting that movement-related signals, rather than causing suppression, may act to shorten it. Our results demonstrate a far-reaching contribution of visual processing mechanisms to saccadic suppression, starting in the retina, without the need to invoke explicit motor-based suppression commands.

Introduction

Saccades are a prominent feature of visual behavior because they allow successive sampling of visual information from the environment. However, from the perspective of the flow of visual information into the brain, these rapid eye movements constitute "disruptive" events, introducing spurious motions that should normally go unnoticed. The question of how and why such perceptual cancelation takes place has intrigued philosophers and scientists for many decades (O'Regan and Noë, 2001). It has been repeatedly found, using a multitude of experiments, that visual sensitivity to brief visual "probes" is strongly impaired around the time of saccades, in a phenomenon known as saccadic suppression (Zuber and Stark, 1966;

Beeler, 1967; Matin, 1974; Riggs and Manning, 1982; Volkmann, 1986; Burr, Morrone and Ross, 1994; Ross, Burr and Morrone, 1996; Bremmer *et al.*, 2009; Hafed and Krauzlis, 2010; Krekelberg, 2010). However, the mechanisms behind such suppression remain controversial. This phenomenon may arise either through internal knowledge of planned eye movements and their associated motor commands (Zuber and Stark, 1966; Duffy and Lombroso, 1968; Diamond, Ross and Morrone, 2000; Ross *et al.*, 2001; Bremmer *et al.*, 2009; Gremmler and Lappe, 2017), or as a result of the visual consequences of retinal image shifts caused by eyeball rotations (Mackay, 1970; Mitrani, Mateeff and Yakimoff, 1971; Matin, Clymer and Matin, 1972; Mitrani, Yakimoff and Mateeff, 1973; Mateeff, Yakimoff and Mitrani, 1976; Brooks, Impelman and Lum, 1981; Macknik and Livingstone, 1998; Castet, S Jeanjean and Masson, 2001; Castet, 2010; García-Pérez and Peli, 2011), and the prevailing view is that internal knowledge of eye movement commands is a necessary prerequisite for saccadic suppression. Here, we were motivated by the fact that the very first visual processing stage in the brain, the retina, possesses rich image processing circuitry that is capable, in principle, of "regularizing" the visual disruptions caused by saccades (Krueger and Fischer, 1973; Noda and Adey, 1974; Barlow *et al.*, 1977; Enroth-Cugell and Jakiela, 1980; Roska and Werblin, 2003; Passaglia, Freeman and Troy, 2009). We therefore asked: how much of the characteristics of perceptual saccadic suppression can be explained by visual-only mechanisms? We found a surprisingly far-reaching contribution of visual processing mechanisms to saccadic suppression, starting in retina, without the need to invoke explicit motor-based suppression commands.

Results

We first asked human subjects to generate saccades across textured backgrounds, akin to how saccades may be made in real life. Subjects viewed coarse or fine textures (Fig. 1A, Methods and Fig. S1). Starting from one of four locations on the display, subjects made 4.8 deg saccades towards display center (Fig. 1A, left). We varied saccade onset and endpoint locations, as well as texture images, across trials to avoid subjects remembering patterns (Methods). At a random time, a luminance pedestal (probe flash) was added to the texture background, for 12 ms, at one of four locations relative to the saccade endpoint (7 deg eccentricity; Fig. 1A, right). We took care to ensure that the retinal region of flash location was stimulated with the background texture (rather than the edge of the monitor or the black surround of the dark laboratory) throughout any given trial (Methods). We also ensured that flash size was larger than the image blobs in the coarse texture, such that average luminance variation within each flash was matched across trials and textures. Coarse and fine textures

had blobs that approximated the sizes of retinal ganglion cell (RGC) or retinal bipolar cell receptive fields, respectively, at the retinal flash locations (Dacey and Petersen, 1992) (Methods).

For both coarse and fine textures, subjects could not localize flashes presented peri-saccadically, thus experiencing strong saccadic suppression (Fig. 1B, C). However, there was clear dependence on texture statistics: saccadic suppression started significantly earlier and recovered significantly later with coarse than fine textures (Fig. 1D; the highlighted time intervals show significant differences between coarse and fine textures at a p-value of $p<0.001$, cluster-based random permutation test (Maris and Oostenveld, 2007; Bellet, Chen and Hafed, 2017), Methods), and this effect was robust across individuals (Fig. S2A). This difference in suppression profiles between textures was not due to the flashes being easier to see over the fine texture without saccades (Fig. S3A, B), and also not due to different saccade kinematics for the different textures (Fig. S3C, D). Thus, saccadic suppression is associated with a visual component directly influencing its strength and time course.

To test if this visual component originates in the retina, we isolated mouse and pig retinae and performed multi-electrode array recordings (Methods). We visually stimulated each retina with coarse and fine textures, matched to ganglion and bipolar cell receptive field sizes in the recorded species (Methods, Fig. S1). We then rapidly translated the textures globally to simulate saccade-like image displacements (Fig. 2A, Methods). Such displacements can robustly activate RGCs, as is evident from the example mouse RGC shown in Fig. 2B. In fact, most recorded RGCs (mouse: 83% of 1,423 cells, pig: 73% of 394 cells) responded robustly to texture displacements, indicating that saccade-induced visual transients in active gaze behavior can constitute strong signals to the retina. Next, at different times relative to texture displacements, we introduced a luminance pedestal (probe flash) to the entire texture for 16 or 33 ms, similar in principle to the perceptual experiments of Fig. 1. Such flashes, when presented in isolation ("baseline"), elicited responses in a sizable fraction of RGCs (mouse: 688/1,423; pig: 228/394). This allowed us to evaluate the consequences of texture displacements on flash responses in these cells, in a way that is conceptually similar to the experiments in Fig. 1, in which we evaluated the consequences of saccades on flash perception. For example, the same RGC of Fig. 2B showed much suppressed neural responses to the flash when it was presented immediately after texture displacements compared to the baseline condition (Fig. 2C, D). These suppressed flash-induced "visual bursts" (Fig. 2D) look remarkably similar to suppressed visual bursts in, say, macaque superior colliculus for stimuli presented after real saccades (Robinson and Wurtz, 1976; Hafed and Krauzlis, 2010; Chen

and Hafed, 2017). Thus, neuronally, there does exist "saccadic suppression" of visual sensitivity at the very first stage of visual processing in the brain, the retina, and it looks qualitatively indistinguishable from saccadic suppression at downstream neural sites (and, indeed, perception).

This retinal "saccadic suppression" had interesting properties. First, RGC suppression did not represent simple activity saturation due to earlier responses to the saccade-like texture displacements as in Fig. 2B. For example, suppression also occurred in RGCs that did not respond strongly to the displacements (Fig. S4A). Rather, suppression was a result of specific spatio-temporal retinal-circuit image processing initiated by the texture displacements. Second, retinal "saccadic suppression" did not critically depend on particular saccade-like profile speeds (Fig. S4B), but it was instead consistent with general stimulus-stimulus interaction effects (Fig. S4C). Most importantly, retinal "saccadic suppression" depended on background texture (Fig. 2E), like in our human experiments (Fig. 1). Specifically, we quantified retinal "saccadic suppression" by calculating a neuronal modulation index (Methods), which is negative for suppressed flash-induced responses: the great majority of RGCs were strongly suppressed during and after texture displacements, with gradual recovery afterwards (Fig. 2E; Fig. S5 shows the underlying population data), and the suppression was more pronounced for coarse than fine textures (Fig. 2E; Fig. S5). These results are consistent with the dependence of human perceptual saccadic suppression on texture statistics (Fig. 1D).

We also found that retinal "saccadic suppression" was a robust phenomenon across many different RGC cell types (Fig. S6). It occurred both in mouse (Fig. 2E, left) and pig (Fig. 2E, right) retinae, two mammalian species with different native oculomotor behavior, different lifestyles, and different eye sizes. Thus, our results so far suggest that the image dependence of perceptual saccadic suppression (Fig. 1) most likely originates in the retina, being the outcome of very general retinal-circuit mechanisms that are conserved across species.

In retina, we not only observed similarities to perceptual saccadic suppression (the presence of retinal suppression, and its dependence on texture statistics), but we additionally noticed that retinal "saccadic suppression" was particularly long lasting (Fig. 2E). We therefore asked our human subjects to maintain fixation while we introduced saccade-like texture displacements in a manner similar to the retinal experiments (Fig. 3A, Methods); brief flashes occurred around the time of these "simulated saccades" exactly like in the first experiment (Fig. 1). This time, due to the absence of real saccades (trials with microsaccades were excluded; Methods), non-visual (motor-related) components could not influence flash-induced neural

responses and their perception. Still, given the retinal results of Fig. 2, we had three hypotheses on what to expect under these conditions, all of which we validated: (1) strong perceptual suppression still occurred regardless of texture details (Fig. 3B, C); (2) suppression strength and duration depended on texture statistics (Fig. 3D); and (3) suppression outlasted the suppression with real saccades (Fig. 3E, F). This last point, in particular, suggests that motor-related signals associated with real saccades (Fig. 1) may act to shorten the perceptual interruption resulting from visually-induced saccadic suppression, while maintaining the putatively retinally-determined (Fig. 2) dependence on image statistics.

In humans, we observed perceptual suppression also prior to saccade-like texture displacements (Mackay, 1970; Mateeff, Yakimoff and Mitrani, 1976) (Fig. 3). This was again consistently dependent on texture statistics (Fig. 3B-D). Critically, making real saccades also shortened such pre-saccadic perceptual suppression relative to when saccades were only simulated using texture displacements (Fig. 3E). Even in our retinal data, we found very slight "pre-saccadic" suppression. However, the effect size was much smaller than for flash responses after texture displacements: the strongest "pre-saccadic" retinal effect occurred at -67 ms with a median population modulation index of -0.024 ($p = 6 \times 10^{-8}$, Wilcoxon signed-rank test) compared to -0.55 ($p = 3 \times 10^{-82}$) for "post-saccadic" suppression at 150 ms delay (Fig. 2E, Fig. S5B). It is therefore likely that this particular phenomenon of perceptual pre-saccadic suppression (Fig. 3B-E) arises not in the retina, but from visual (not movement-command-related) processing further downstream, perhaps through backwards masking (Macknik and Livingstone, 1998; Breitmeyer, 2007).

Our results so far suggest that visual contributions go a long way in explaining properties of perceptual saccadic suppression. We therefore wondered whether such contributions can also explain classic suppression phenomena when uniform, rather than textured, backgrounds are used. One such robust phenomenon has been the selective suppression of low spatial frequencies. In a classic study (Burr, Morrone and Ross, 1994), subjects viewed briefly flashed gratings over a uniform background. Around the time of saccades, visibility of low-spatial frequency gratings was suppressed much more strongly than of high-frequency gratings, and this was interpreted as a motor-related influence on magnocellular pathways (Diamond, Ross and Morrone, 2000; Ross *et al.*, 2001). Still, convincing neural mechanisms for this phenomenon remain elusive (Castet, S Jeanjean and Masson, 2001; Castet, Sébastien Jeanjean and Masson, 2001; Ramcharan, Gnadt and Sherman, 2001; Reppas, Usrey and Reid, 2002; Kleiser, Seitz and Krekelberg, 2004; Royal *et al.*, 2006; Hass and Horwitz, 2011; Chen and Hafed, 2017). Can our results so far, highlighting the prominence of visual mechanisms

underlying saccadic suppression, also account for this classic phenomenon? The answer lies in considering this phenomenon from the perspective of visual input during such experiments: saccades across a uniform background invariably involve moving the image of the video monitor (or other form of display) across the retina. Therefore, the image of any edge discontinuity associated with the display monitor (or with the surrounding cardboard paper around it (Burr, Morrone and Ross, 1994)) will invariably move because of the saccade. This allows us to ask if one can replicate selective suppression of low spatial frequencies (Burr, Morrone and Ross, 1994) without any saccades at all, solely based on the visual flow experienced during such experiments.

We first replicated the classic phenomenon itself. Our subjects localized briefly flashed vertical Gabor gratings with different spatial frequencies (Methods); the flashes occurred peri-saccadically as in Fig. 1A. Here, however, the screen was a homogeneous gray, like in the classic experiment, with the exception of a surround region showing a stationary texture (the coarse texture used in our earlier experiments) (Fig. 4A). We call the large homogeneous central region of the screen (diameter: 20 deg) the “virtual monitor”. The outcome confirmed the classic findings: Fig. 4B (left) shows localization performance for flashed gratings around saccade onset, compared to flashes without saccades (and without any other display transients; Methods), and Fig. 4B (right) plots the ratio of those percepts. Perception of low spatial frequency gratings was selectively suppressed (relevant statistics are shown in Fig. 4). Full time courses of these effects are shown in Figs. S7, S8.

The presence of the textured surround allowed us to next isolate the effects of visual flow during these experiments. In separate trials, we asked subjects to fixate, and we presented saccade-like image motion. For example, the virtual monitor moved together with its textured surround from the top left corner towards display center (Fig. 4C), in order to simulate a real saccade from the lower right corner to display center (Fig. 4A). We then briefly presented the same Gabor gratings as in Fig. 4A, B. Relative to fixation position, this experiment was comparable to the situation with real saccades: there was a uniform background against which a brief Gabor grating was flashed. And, indeed, we observed the same selective suppression of low spatial frequencies despite the absence of saccades (Fig. 4D). Moreover, again consistent with our results from Figs. 1-3, the suppression with simulated saccades lasted longer than with real saccades (robust selective suppression in Fig. 4D occurred even 84 ms after simulated saccades; Fig. S7). Similar results were obtained with a uniform black surround around the virtual monitor, as might be the case in typical laboratory settings (Fig. S8). Therefore, visual mechanisms account even for the results of (Burr, Morrone and Ross, 1994)

and similar experiments (Chen and Hafed, 2017) using uniform backgrounds, without the need to invoke non-visual (motor-related) mechanisms.

Motivated by the differences between coarse and fine textures in Figs. 1-3, we next replaced the coarse texture around the virtual monitor (Fig. 4A, C) with a fine texture, and we repeated the same experiments with simulated saccades (Fig. 4F). In this case, surprisingly, we observed uniform suppression of gratings of all spatial frequencies (Fig. 4F). This led us to make a strong prediction: if saccadic suppression properties do indeed rely on visual processing, then suppression during real saccades should depend mainly on visual context, and one should be able to easily violate the classic phenomenon (namely, the specific suppression of low spatial frequencies (Burr, Morrone and Ross, 1994)). This is exactly what we found (Fig. 4E): for real saccades across the virtual monitor, and with the surrounding visual context being a fine rather than coarse texture, we observed perceptual suppression for all gratings, abolishing suppression selectivity for low spatial frequencies (Burr, Morrone and Ross, 1994). In all cases, the effects were not explained by motor variability across surround texture conditions (Fig. S3E, F).

Therefore, either with or without real saccades, perceptual saccadic suppression always occurred, simply as a function of visual flow (Figs. 1, 3, 4). Such suppression quantitatively depended on scene statistics, both for full-field textures (Figs. 1, 3) in a manner predicted by retinal processing (Fig. 2), and for textures limited to the surround (Fig. 4). Even the selectivity of suppression for low spatial frequencies (Burr, Morrone and Ross, 1994) was determined by visual context (Fig. 4).

Conclusion

Taken together, our results indicate that visual image processing accounts for a large component of classic perceptual demonstrations of saccadic suppression, and that such image processing occurs as early as in the very first stage of visual processing, the retina. Motor-related mechanisms seem to be equally important, though, since they appear to shorten pre- and post-saccadic suppression originating from visual mechanisms (Fig. 3), and therefore minimize the duration of saccade-induced disruptions. Furthermore, information contained in the motor command is likely critical for adjustments of spatial receptive fields across saccades in parietal and frontal cortices (Duhamel, Colby and Goldberg, 1992; Sommer and Wurtz, 2006). Our findings leave open the possibility, however, that transsaccadic image flow might play a role in this phenomenon as well.

References

Barlow, H. B. *et al.* (1977) 'The effects of remote retinal stimulation on the responses of cat retinal ganglion cells.', *The Journal of Physiology*, 269(1), pp. 177–194. doi: 10.1113/jphysiol.1977.sp011898.

Beeler, G. W. (1967) 'Visual threshold changes resulting from spontaneous saccadic eye movements', *Vision Research*, 7(9–10), pp. 769–775. doi: 10.1016/0042-6989(67)90039-9.

Bellet, J., Chen, C.-Y. and Hafed, Z. M. (2017) 'Sequential hemifield gating of α- and β-behavioral performance oscillations after microsaccades', *Journal of Neurophysiology*. American Physiological Society, 118(5), pp. 2789–2805. doi: 10.1152/jn.00253.2017.

Breitmeyer, B. G. (2007) 'Visual masking: past accomplishments, present status, future developments', *Advances in Cognitive Psychology*, 3(1), pp. 9–20. doi: 10.2478/v10053-008-0010-7.

Bremmer, F. *et al.* (2009) 'Neural dynamics of saccadic suppression', *Journal of Neuroscience*, 29(40), pp. 12374–12383. doi: 10.1523/JNEUROSCI.2908-09.2009.

Brooks, B. A., Impelman, D. M. K. and Lum, J. T. (1981) 'Backward and forward masking associated with saccadic eye movement', *Perception & Psychophysics*, 30(1), pp. 62–70. doi: 10.3758/BF03206137.

Burr, D. C., Morrone, M. C. and Ross, J. (1994) 'Selective suppression of the magnocellular visual pathway during saccadic eye movements', *Nature*, 371(6497), pp. 511–513. doi: 10.1038/371511a0.

Castet, E. (2010) 'Perception of intra-saccadic motion', in *Dynamics of visual motion processing*. Boston, MA: Springer US, pp. 141–160. doi: 10.1007/978-1-4419-0781-3.

Castet, E., Jeanjean, S. and Masson, G. S. (2001) ''Saccadic suppression'- no need for an active extra-retinal mechanism.', *Trends in neurosciences*, 24(6), pp. 317–318. doi: 10.1016/S0166-2236(00)01827-0.

Castet, E., Jeanjean, S. and Masson, G. S. (2001) '"Saccadic suppression" – no need for an active extra-retinal mechanism', *Trends in Neurosciences*, 24(6), pp. 316–317. doi: 10.1016/S0166-2236(00)01828-2.

Chen, C.-Y. and Hafed, Z. M. (2013) ‘Postmicrosaccadic Enhancement of Slow Eye Movements’, *Journal of Neuroscience*, 33(12), pp. 5375–5386. doi: 10.1523/JNEUROSCI.3703-12.2013.

Chen, C.-Y. and Hafed, Z. M. (2017) ‘A neural locus for spatial-frequency specific saccadic suppression in visual-motor neurons of the primate superior colliculus’, *Journal of Neurophysiology*, 117(4), pp. 1657–1673. doi: 10.1152/jn.00911.2016.

Dacey, D. M. and Petersen, M. R. (1992) ‘Dendritic field size and morphology of midget and parasol ganglion cells of the human retina.’, *Proceedings of the National Academy of Sciences*, 89(20), pp. 9666–9670. doi: 10.1073/pnas.89.20.9666.

Diamond, M. R., Ross, J. and Morrone, M. C. (2000) ‘Extraretinal control of saccadic suppression.’, *The Journal of neuroscience : the official journal of the Society for Neuroscience*, 20(9), pp. 3449–3455. doi: 10.1523/JNEUROSCI.20-09-03449.2000.

Diggelmann, R. *et al.* (2018) ‘Automatic spike sorting for high-density microelectrode arrays’, *Journal of Neurophysiology*, 120(6), pp. 3155–3171. doi: 10.1152/jn.00803.2017.

Duffy, F. H. and Lombroso, C. T. (1968) ‘Electrophysiological evidence for visual suppression prior to the onset of a voluntary saccadic eye movement.’, *Nature*, 218(5146), pp. 1074–1075. doi: 10.1038/2181074a0.

Duhamel, J. R., Colby, C. L. and Goldberg, M. E. (1992) ‘The updating of the representation of visual space in parietal cortex by intended eye movements.’, *Science (New York, N.Y.)*, 255(5040), pp. 90–2. Available at: http://www.sciencemag.org/content/255/5040/90.short (Accessed: 30 July 2014).

Enroth-Cugell, C. and Jakiela, H. G. (1980) ‘Suppression of cat retinal ganglion cell responses by moving patterns.’, *The Journal of Physiology*, 302(1), pp. 49–72. doi: 10.1113/jphysiol.1980.sp013229.

Farrow, K. *et al.* (2013) ‘Ambient Illumination Toggles a Neuronal Circuit Switch in the Retina and Visual Perception at Cone Threshold’, *Neuron*. Elsevier Inc., 78(2), pp. 325–338. doi: 10.1016/j.neuron.2013.02.014.

Frey, U. *et al.* (2009) ‘Microelectronic system for high-resolution mapping of extracellular

electric fields applied to brain slices', *Biosensors and Bioelectronics*, 24(7), pp. 2191–2198. doi: 10.1016/j.bios.2008.11.028.

García-Pérez, M. A. and Peli, E. (2011) 'Visual contrast processing is largely unaltered during saccades', *Frontiers in Psychology*, 2(SEP), pp. 1–15. doi: 10.3389/fpsyg.2011.00247.

Gremmler, S. and Lappe, M. (2017) 'Saccadic suppression during voluntary versus reactive saccades', *Journal of Vision*, 17(8), pp. 1–10. doi: 10.1167/17.8.8.doi.

Grujic, N. *et al.* (2018) 'Perisaccadic perceptual mislocalization is different for upward saccades', *Journal of Neurophysiology*, 120(6), pp. 3198–3216. doi: 10.1152/jn.00350.2018.

Hafed, Z. M. (2013) 'Alteration of Visual Perception prior to Microsaccades', *Neuron*. Elsevier Inc., 77(4), pp. 775–786. doi: 10.1016/j.neuron.2012.12.014.

Hafed, Z. M. and Krauzlis, R. J. (2010) 'Microsaccadic suppression of visual bursts in the primate superior colliculus.', *The Journal of neuroscience : the official journal of the Society for Neuroscience*, 30(28), pp. 9542–9547. doi: 10.1523/JNEUROSCI.1137-10.2010.

Hass, C. A. and Horwitz, G. D. (2011) 'Effects of microsaccades on contrast detection and V1 responses in macaques', *Journal of Vision*, 11(3), pp. 3–3. doi: 10.1167/11.3.3.

Idrees, S. *et al.* (2016) 'UnitBrowser - A Tool to Evaluate and Post-Process Units Sorted by Automatic Spike Sorting Algorithms', *Frontiers in Neuroscience*, 10. doi: 10.3389 / conf.fnins.2016.93.00054.

Kleiser, R., Seitz, R. J. and Krekelberg, B. (2004) 'Neural correlates of saccadic suppression in humans', *Current Biology*, 14(5), pp. 386–390. doi: 10.1016/j.cub.2004.02.036.

Krekelberg, B. (2010) 'Saccadic suppression', *Current Biology*, 20(5), pp. R228–R229. doi: 10.1016/j.cub.2009.12.018.

Krueger, J. and Fischer, B. (1973) 'Strong periphery effect in cat retinal ganglion cells. Excitatory responses in ON- and OFF-center neurones to single grid displacements', *Experimental Brain Research*, 18(3), pp. 316–318. doi: 10.1007/BF00234601.

Mackay, D. M. (1970) 'Elevation of visual threshold by displacement of retinal image.', *Nature*, 225(5227), pp. 90–92. doi: 10.1038/225090a0.

Macknik, S. L. and Livingstone, M. S. (1998) ‘Neuronal correlates of visibility and invisibility in the primate visual system’, *Nature Neuroscience*, 1(2), pp. 144–149. doi: 10.1038/393.

Maris, E. and Oostenveld, R. (2007) ‘Nonparametric statistical testing of EEG- and MEG-data’, *Journal of Neuroscience Methods*, 164(1), pp. 177–190. doi: 10.1016/j.jneumeth.2007.03.024.

Mateeff, S., Yakimoff, N. and Mitrani, L. (1976) ‘Some characteristics of the visual masking by moving contours’, *Vision Research*, 16(5), pp. 489–492. doi: 10.1016/0042-6989(76)90027-4.

Matin, E. (1974) ‘Saccadic suppression: a review and an analysis.’, *Psychological bulletin*, 81(12), pp. 899–917. Available at: http://www.ncbi.nlm.nih.gov/pubmed/4612577.

Matin, E., Clymer, A. B. and Matin, L. (1972) ‘Metacontrast and saccadic suppression.’, *Science (New York, N.Y.)*, 178(4057), pp. 179–182. doi: 10.1126/science.178.4057.179.

Mitrani, L., Mateeff, S. and Yakimoff, N. (1971) ‘Is saccadic suppression really saccadic?’, *Vision Research*, 11(10), pp. 1157–1161. doi: 10.1016/0042-6989(71)90119-2.

Mitrani, L., Yakimoff, N. and Mateeff, S. (1973) ‘Saccadic suppression in the presence of structured background’, *Vision Research*, 13(2), pp. 517–521. doi: 10.1016/0042-6989(73)90135-1.

Müller, J. *et al.* (2015) ‘High-resolution CMOS MEA platform to study neurons at subcellular, cellular, and network levels’, *Lab on a Chip*. Royal Society of Chemistry, 15(13), pp. 2767–2780. doi: 10.1039/C5LC00133A.

Münch, T. A. *et al.* (2009) ‘Approach sensitivity in the retina processed by a multifunctional neural circuit’, *Nature Neuroscience*, 12(10), pp. 1308–1316. doi: 10.1038/nn.2389.

Noda, H. and Adey, W. R. (1974) ‘Retinal ganglion cells of the cat transfer information on saccadic eye movement and quick target motion’, *Brain Research*, 70(2), pp. 340–345. doi: 10.1016/0006-8993(74)90323-0.

O’Regan, J. K. and Noë, A. (2001) ‘A sensorimotor account of vision and visual consciousness’, *Behavioral and Brain Sciences*, 24(05), pp. 939–973. doi:

10.1017/S0140525X01000115.

Passaglia, C. L., Freeman, D. K. and Troy, J. B. (2009) ‘Effects of remote stimulation on the modulated activity of cat retinal ganglion cells.’, *The Journal of neuroscience : the official journal of the Society for Neuroscience*, 29(8), pp. 2467–2476. doi: 10.1523/JNEUROSCI.4110-08.2009.

Peli, E. *et al.* (1993) ‘Contrast sensitivity to patch stimuli: effects of spatial bandwidth and temporal presentation.’, *Spatial vision*, 7(1), pp. 1–14. doi: 10.1163/156856893X00018.

Ramcharan, E. J., Gnadt, J. W. and Sherman, S. M. (2001) ‘The effects of saccadic eye movements on the activity of geniculate relay neurons in the monkey’, *Visual Neuroscience*. UB Tubingen, 18(2), pp. 253–258. doi: 10.1017/S0952523801182106.

Reinhard, K. *et al.* (2014) ‘Step-By-Step Instructions for Retina Recordings with Perforated Multi Electrode Arrays’, *PLoS ONE*. Edited by S. Barnes, 9(8), p. e106148. doi: 10.1371/journal.pone.0106148.

Reppas, J. B., Usrey, W. M. and Reid, R. C. (2002) ‘Saccadic eye movements modulate visual responses in the lateral geniculate nucleus.’, *Neuron*, 35(5), pp. 961–974. doi: 10.1016/S0896-6273(02)00823-1.

Riggs, L. A. and Manning, K. A. (1982) ‘Saccadic suppression under conditions of whiteout.’, *Investigative ophthalmology & visual science*, 23(1), pp. 138–143. Available at: http://www.ncbi.nlm.nih.gov/pubmed/7085217.

Robinson, D. L. and Wurtz, R. H. (1976) ‘Use of an extraretinal signal by monkey superior colliculus neurons to distinguish real from self-induced stimulus movement’, *Journal of Neurophysiology*, 39(4), pp. 852–870. doi: 10.1152/jn.1976.39.4.852.

Roska, B. and Werblin, F. (2003) ‘Rapid global shifts in natural scenes block spiking in specific ganglion cell types’, *Nature Neuroscience*, 6(6), pp. 600–608. doi: 10.1038/nn1061.

Ross, J. *et al.* (2001) ‘Changes in visual perception at the time of saccades’, *Trends in Neurosciences*, 24(2), pp. 113–121. doi: 10.1016/S0166-2236(00)01685-4.

Ross, J., Burr, D. C. and Morrone, M. C. (1996) ‘Suppression of the magnocellular pathway during saccades.’, *Behavioural brain research*, 80(1–2), pp. 1–8. doi: 10.1016/0166-

4328(96)00012-5.

Royal, D. W. *et al.* (2006) ‘Correlates of motor planning and postsaccadic fixation in the macaque monkey lateral geniculate nucleus’, *Experimental Brain Research*, 168(1–2), pp. 62–75. doi: 10.1007/s00221-005-0093-z.

Sakatani, T. and Isa, T. (2007) ‘Quantitative analysis of spontaneous saccade-like rapid eye movements in C57BL/6 mice’, *Neuroscience Research*, 58(3), pp. 324–331. doi: 10.1016/j.neures.2007.04.003.

Schütt, H. H. *et al.* (2016) ‘Painfree and accurate Bayesian estimation of psychometric functions for (potentially) overdispersed data’, *Vision Research*, 122, pp. 105–123. doi: 10.1016/j.visres.2016.02.002.

Schwartz, G. W. *et al.* (2012) ‘The spatial structure of a nonlinear receptive field’, *Nature Neuroscience*. Nature Publishing Group, 15(11), pp. 1572–1580. doi: 10.1038/nn.3225.

Sommer, M. A. and Wurtz, R. H. (2006) ‘Influence of the thalamus on spatial visual processing in frontal cortex’, *Nature*, 444(7117), pp. 374–377. doi: 10.1038/nature05279.

Tikidji-Hamburyan, A. *et al.* (2015) ‘Retinal output changes qualitatively with every change in ambient illuminance’, *Nature Neuroscience*. Nature Publishing Group, 18(1), pp. 66–74. doi: 10.1038/nn.3891.

Volkmann, F. C. (1986) ‘Human visual suppression’, *Vision Research*, 26(9), pp. 1401–1416. doi: 10.1016/0042-6989(86)90164-1.

Zhang, Y. *et al.* (2012) ‘The most numerous ganglion cell type of the mouse retina is a selective feature detector’, *Proceedings of the National Academy of Sciences*, 109(36), pp. E2391–E2398. doi: 10.1073/pnas.1211547109.

Zuber, B. L. and Stark, L. (1966) ‘Saccadic suppression: Elevation of visual threshold associated with saccadic eye movements’, *Experimental Neurology*, 16(1), pp. 65–79. doi: 10.1016/0014-4886(66)90087-2.

Acknowledgements: We thank Andreas Hierlemann for providing the HiDens CMOS MEA system and helping us to establish our high-density MEA recordings. We also thank Roland Diggelmann for help in setting up the pipeline (including providing code) for automatic spike sorting of high-density MEA recordings. This work was supported by funds of the Deutsche Forschungsgemeinschaft (DFG) to the Werner Reichardt Center for Integrative Neuroscience (EXC 307) and to T.A.M. (MU3792/3-1). T.A.M. received support from the Tistou and Charlotte Kerstan Foundation. T.A.M. and Z.M.H. were also supported by an intra-mural funding program (Projekt 2013-05) of the Werner Reichardt Centre for Integrative Neuroscience. F.F. was supported through a Swiss National Science Foundation Ambizione grant (PZ00P3_167989).

Author contributions: S.I., M.B., T.A.M., Z.M.H. designed the overall study; S.I., M.B., T.A.M., Z.M.H. designed experiments; S.I. performed ex vivo retina experiments; M.B., Z.M.H. performed human psychophysics experiments; S.I., M.B., F.F., T.A.M., Z.M.H. analyzed data; S.I., M.B., F.F., T.A.M., Z.M.H. wrote manuscript.

Competing interests: The authors declare no competing interests.

Data and materials availability: All data are stored and archived on secure institute computers, and they are available upon reasonable request.

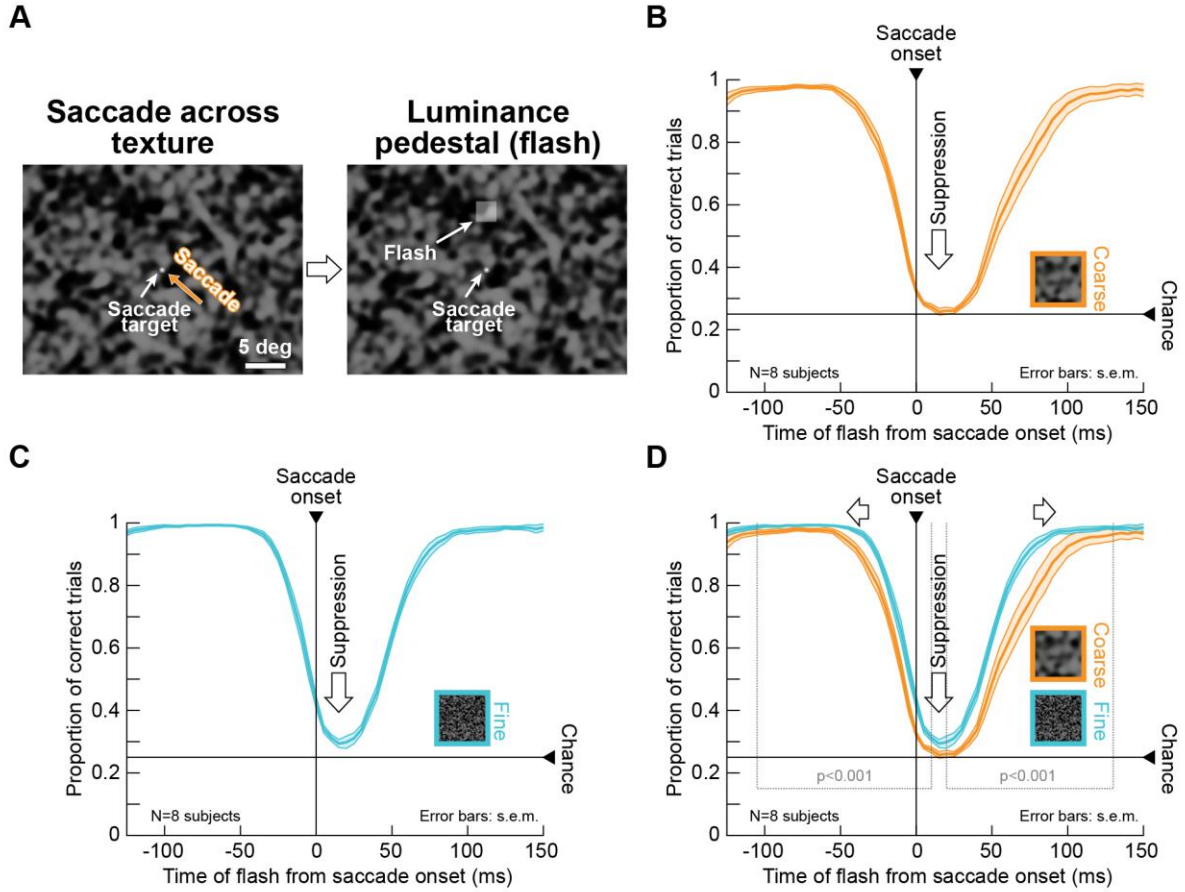

Fig. 1. Image dependence of perceptual saccadic suppression. (A) Human subjects generated saccades from one of four diagonal locations towards display center (here: from the lower right). A luminance pedestal was flashed peri-saccadically at one of four locations around display center (right, left, up, or down; here: up). The example shows the coarse background texture (insets in **C**, **D** show fine textures for comparison; also see Fig. S1 and Methods). **(B, C)** Subjects failed to localize peri-saccadic flashes with both coarse **(B)** and fine **(C)** textures (we binned perceptual reports as a function of flash time from saccade onset using 50-ms bins moved in steps of 5 ms). **(D)** However, perceptual suppression started earlier and lasted longer with a coarse background. The highlighted time points ($p<0.001$) denote significantly different time clusters between the coarse and fine conditions (Methods). Curves show averages (+/- s.e.m. bounds) of individual subjects' suppression curves. Figures S2, S3 show individual subject results, as well as controls for flash visibility (in the absence of saccades) and saccade motor variability.

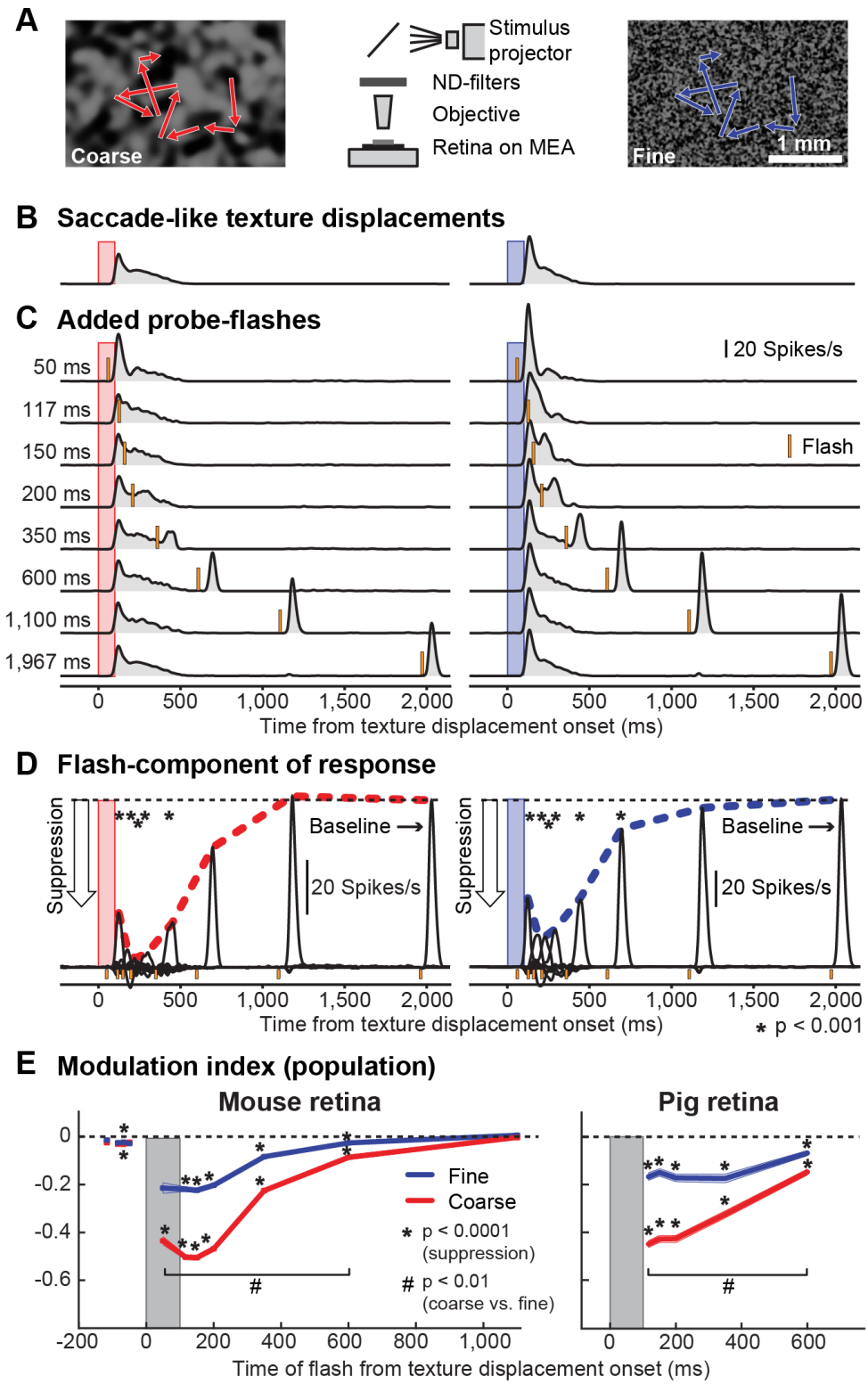

Fig. 2. "Saccadic suppression" in retina. **(A)** We recorded RGC activity from ex-vivo retinae placed on multielectrode arrays (MEA). A coarse (left) or fine (right) texture was repeatedly translated in a saccade-like manner (red or blue "scan paths"), and we presented brief visual flashes at different times relative to "saccades" (similar to Fig. 1). **(B, C)** Average activity of an example RGC to 39 texture displacements alone **(B)** or followed by probe flashes at different time delays **(C)**. Red and blue bars show the timings of the texture displacements; orange bars indicate probe flashes. Flash-induced responses were strongly suppressed immediately following saccade-like texture displacements. **(D)** This effect is

isolated by subtracting responses in **B** from those in **C**. Dashed colored lines highlight the time courses of retinal "saccadic" suppression relative to baseline flash-induced responses. **(E)** Modulation index highlighting retinal "saccadic suppression" (Methods; negative values indicate suppressed flash-induced neural responses). Both mouse and pig retinae showed strong suppression during and after texture displacements, which also depended on texture statistics (similar to perception; Fig. 1). Error bars denote s.e.m., and asterisks/hashes indicate statistical significance (Methods). The numbers of recorded cells at each flash time in **E** were as follows. Mouse RGCs: N=179 (-177 ms, -84 ms, -50 ms), 161 (-67 ms), 136 (50 ms), 527 (117 ms), 520 (150 ms), 502 (200 ms, 600 ms), 688 (350 ms), 345 (1,100 ms); pig RGCs: N=228 for each time point. Figures S4-S6 show additional properties of retinal "saccadic suppression", and the population data underlying panel **E**.

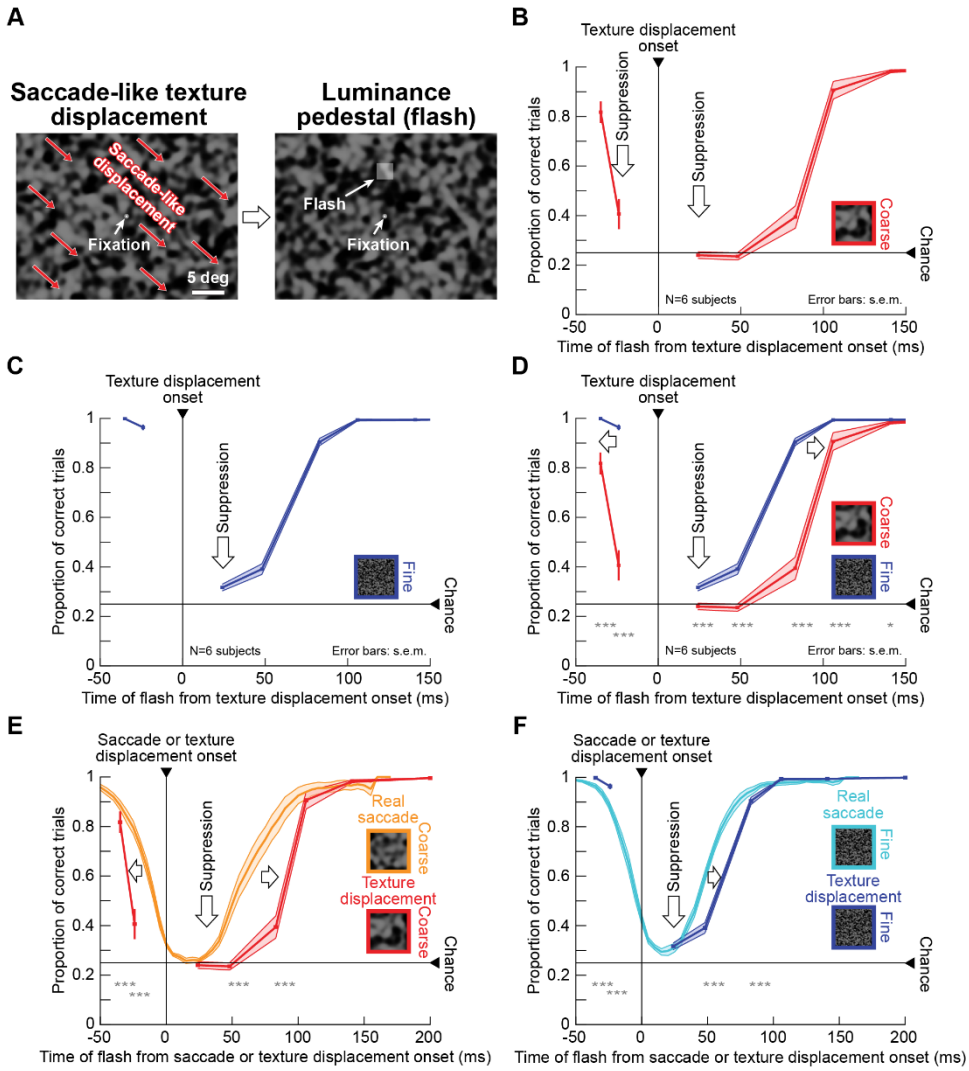

Fig. 3. Image dependence of perceptual suppression without saccades. (A) Rapid texture displacements simulated saccade-like image displacements, similar to the retina experiments (Fig. 2). We used the same flashes and "simulated" saccade directions as in Fig. 1. The example shows a coarse texture (fine textures are shown in insets in **C**, **D**, and **F**). **(B, C)** Pre-, peri-, and post-displacement perceptual suppression occurred for both coarse **(B)** and fine **(C)** textures without "real" saccades. **(D)** As with real saccades (Fig. 1), suppression started earlier and lasted longer with coarse textures (also compare to similar retinal effects in Fig. 2E). Notably, pre-displacement suppression depended on texture statistics, just like with real saccades (Fig. 1). **(E, F)** Texture displacements were associated with significantly longer suppression than real saccades. For coarse textures (which were most effective in causing suppression overall), flashes presented before real or simulated saccades were suppressed earlier in the simulated saccade condition than in the real saccade condition; thus, prolonged suppression with texture displacements was not restricted to post-displacement flashes only. Error bars denote s.e.m. across individual subjects' curves. Asterisks denote significant differences between coarse and fine textures **(D)** or between real and simulated saccades **(E, F)** at each indicated time point (χ^2 tests with Bonferroni corrections; * $p<0.005$ in **D** and $p<0.007$ in **E**,**F**; *** $p<0.0001$ in **D** and $p<0.00014$ in **E**,**F**). Figure S2 shows individual subject results.

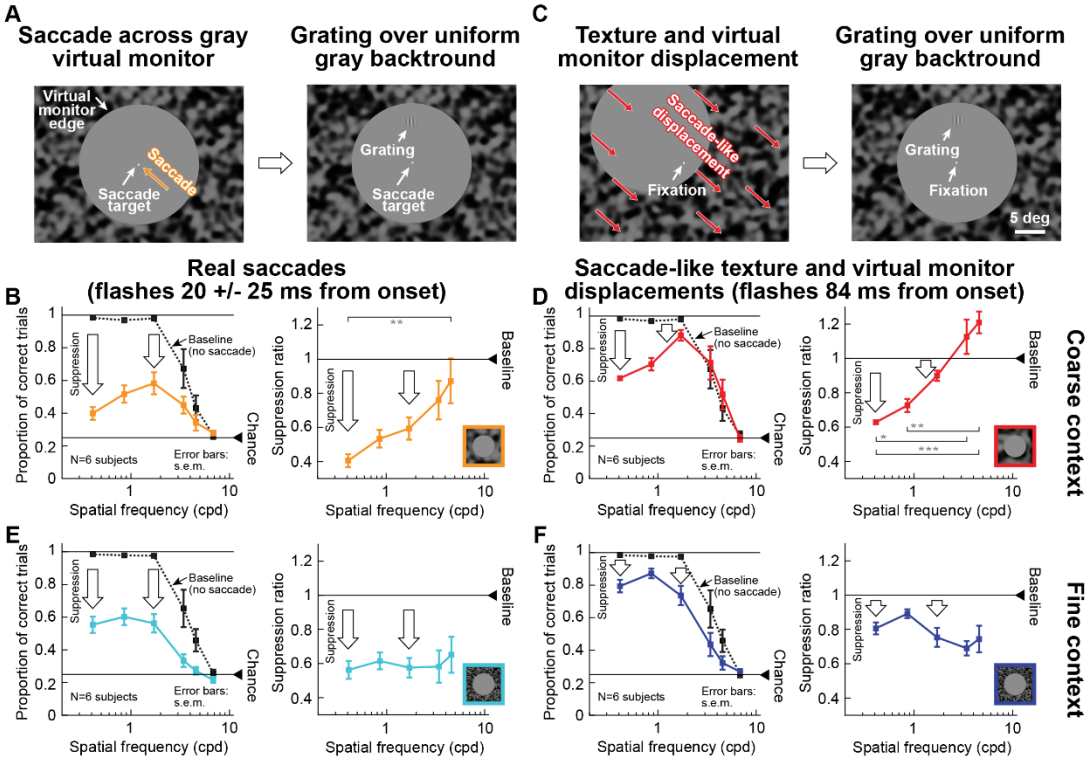

Fig. 4. Selective peri-saccadic suppression of low spatial frequencies (Burr, Morrone and Ross, 1994) **is a visual phenomenon. (A)** Left: Subjects made saccades towards display center. Right: brief gratings were presented peri-saccadically over a uniform gray background (circular "virtual monitor" surrounded by a texture; saccade directions and flash locations were similar to Figs. 1, 3). The example shown is for a coarse texture. **(B)** Left: proportion of correct localizations of gratings having different spatial frequencies during fixation ("Baseline"; dashed curve) and for peri-saccadic flashes (solid curve). Consistent with (Burr, Morrone and Ross, 1994), low spatial frequencies were associated with the strongest suppression relative to baseline. Right: ratio of peri-saccadic to baseline performance (highest spatial frequency not shown because it was at chance performance even in baseline). Suppression depended on grating spatial frequency (χ^2=13.46, p=0.0092, df=4; Kruskal-Wallis test; ** p<0.01 for post-hoc pairwise comparisons between the lowest and highest spatial frequencies). **(C)** Left: we simulated saccade-induced image displacements by translating the virtual monitor and surrounding texture from one corner towards display center. Right: gratings as in **A** appeared (Methods). **(D)** The same selective suppression of low spatial frequencies as in **B** occurred when saccades were replaced by virtual monitor and texture displacements. "Baseline" in this context means both no saccades and also no virtual monitor and texture displacements. Suppression ratio depended on spatial frequency (χ^2=25.33, p<0.0001, df=4, Kruskal-Wallis test; * p<0.05, ** p<0.01, *** p<0.001 for post-hoc pairwise comparisons between individual spatial frequencies). **(E, F)** With a fine, rather than coarse, surround texture, both real **(E)** and simulated **(F)** saccades were associated with suppression for all spatial frequencies; suppression selectivity (Burr, Morrone and Ross, 1994) was eliminated (χ^2=0.8,p=0.938, df=4 for **e** and χ^2=7.74, p=0.102, df=4 for **F**, Kruskal-Wallis test). Error bars denote. s.e.m. across individual subjects' curves. Figures. S7, S8 show full time courses as well as controls with black surrounds around the virtual monitor. Note that in **D**, **F**, we exploited the longer time course of visual suppression (Figs. 3, S7) to probe perception at a later time than in **B**, **E**.

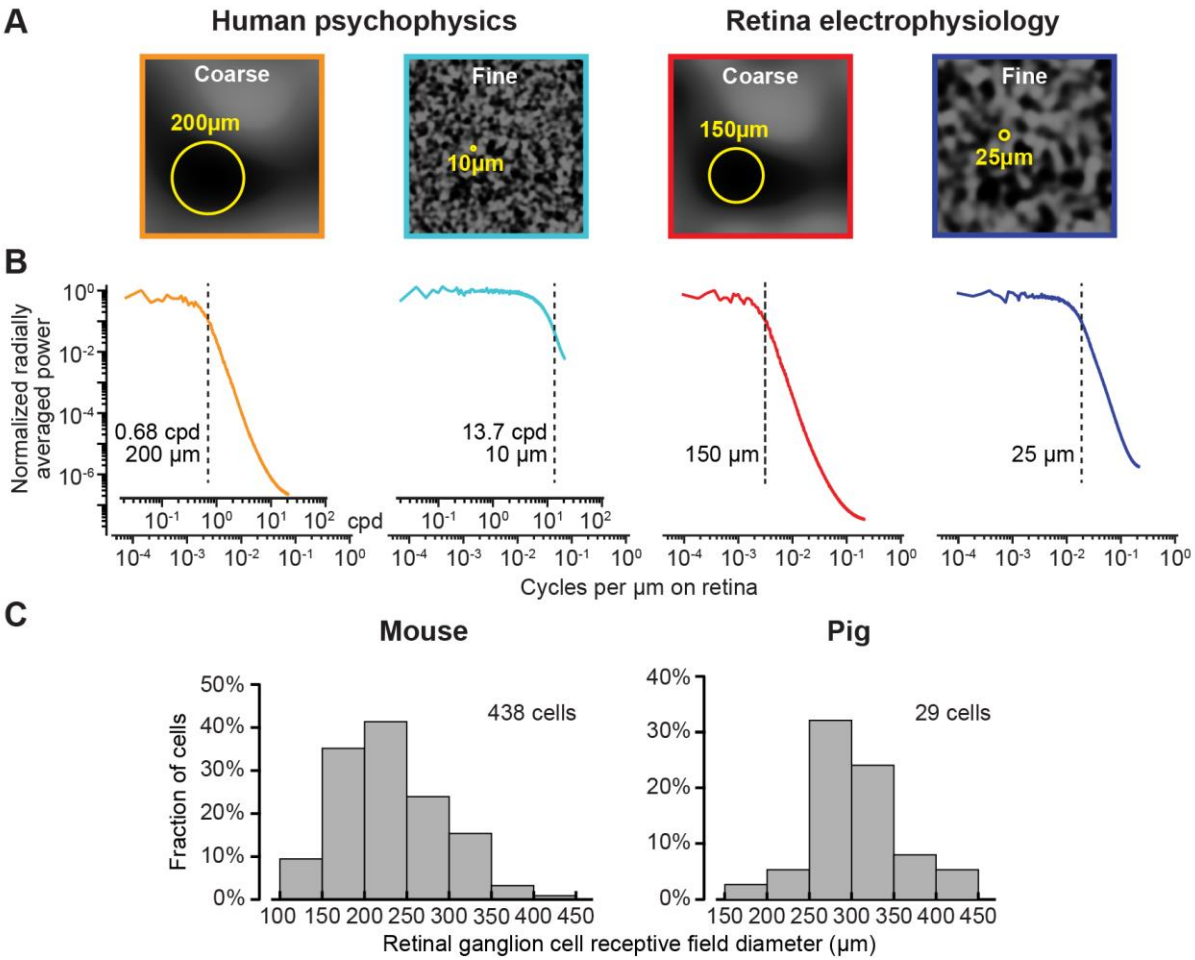

Fig. S1. Textured backgrounds tailored to receptive field sizes of retinal ganglion (coarse) or bipolar (fine) cells in the different species that we studied. (A) We created textures by convolving random binary pixel images with a Gaussian blurring filter. We varied the σ parameter of the Gaussian blurring filter (Methods) to define a so-called "spatial scale" for a given texture (indicated as yellow circles in the examples shown). For each species, we picked the spatial scale to result in dark or bright image blobs that approximated the sizes of either retinal ganglion (coarse) or bipolar (fine) cell receptive fields, and we then set σ to half the "spatial scale" value (Methods). **(B)** We computed radially-averaged power spectra for textures like in **A**, normalized to the maximum average power. Low-pass characteristics in all spatial scales were clear, as expected: less than 5% of the total average power was above the spatial frequency corresponding to the specific spatial scale of a given texture (vertical dashed lines). The inset x-axes in the first two spectra (used for human perceptual experiments) show units of cycles per degree (cpd) in addition to cycles per µm on the retina. **(C)** Histograms showing the distributions of receptive field diameters (Methods) in mouse (left) and pig (right) retinal ganglion cells that we recorded. Since the distributions were generally similar, we used the same spatial scale parameter for the retinal recordings in both species. Human spatial scale parameters were estimated based on human receptive field diameters from the literature (Methods).

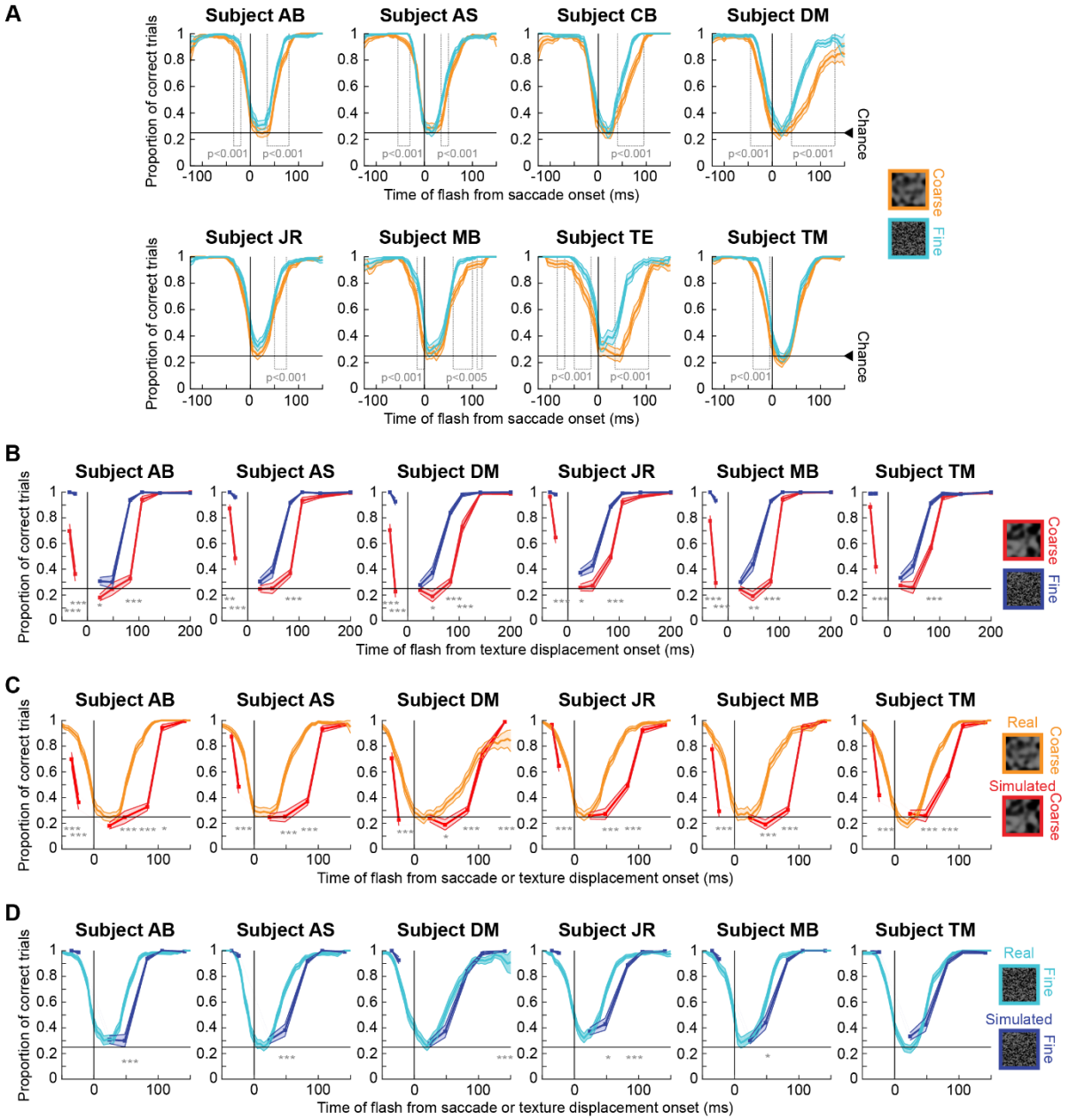

Fig. S2 Individual subject results from the perceptual experiments of Figs. 1, 3. (A) Identical analyses to Fig. 1D, but now shown separately for each individual subject. Error bars in this case denote s.e.m. across trials. All subjects experienced strong saccadic suppression, going from perfect localization performance to near-chance performance at peak suppression. Moreover, using strict statistical criteria (indicated in the figure and described in detail in Methods), all subjects had significant time clusters during which perception was different between saccadic suppression for saccades generated across coarse or fine textures. **(B)** Same analyses as in Fig. 3D, but now showing individual subject results when saccades were replaced by saccade-like texture displacements during fixation. All subjects showed prolonged suppression after coarse texture displacements than after fine texture displacements; all subjects also showed earlier and stronger "pre-saccadic" suppression for coarse textures. Note that this "pre-saccadic" effect is purely visual, since the subjects never made saccades in this condition. Also, note that all subjects who participated in this experiment had also participated in the version with real saccades in **A**. Therefore, whether with or without saccades, perceptual suppression depended on image statistics. **(C, D)** Comparisons of perceptual suppression between real and "simulated" saccades across coarse **(C)** and fine **(D)** textures, as

in Fig. 3E, F but now separating data from individual subjects. Note how even pre-saccadic suppression was prolonged in simulated relative to real saccades (i.e. started earlier in simulated saccades) in the coarse texture condition, which was most effective in causing suppression overall. Error bars in all cases denote s.e.m. across trials. Asterisks in **B** denote a significant difference between coarse and fine conditions at the indicated flash time (χ^2 tests with Bonferroni corrections; * $p<0.005$, ** $p<0.001$, *** $p<0.0001$). Asterisks in **C**, **D** denote significant differences (* $p<0.007$, ** $p<0.0014$, *** $p<0.00014$) between real and simulated saccades, comparing perception of a flash at the indicated time delay after simulated saccades to the corresponding time bin (+/- 25 ms) from the real saccade condition.

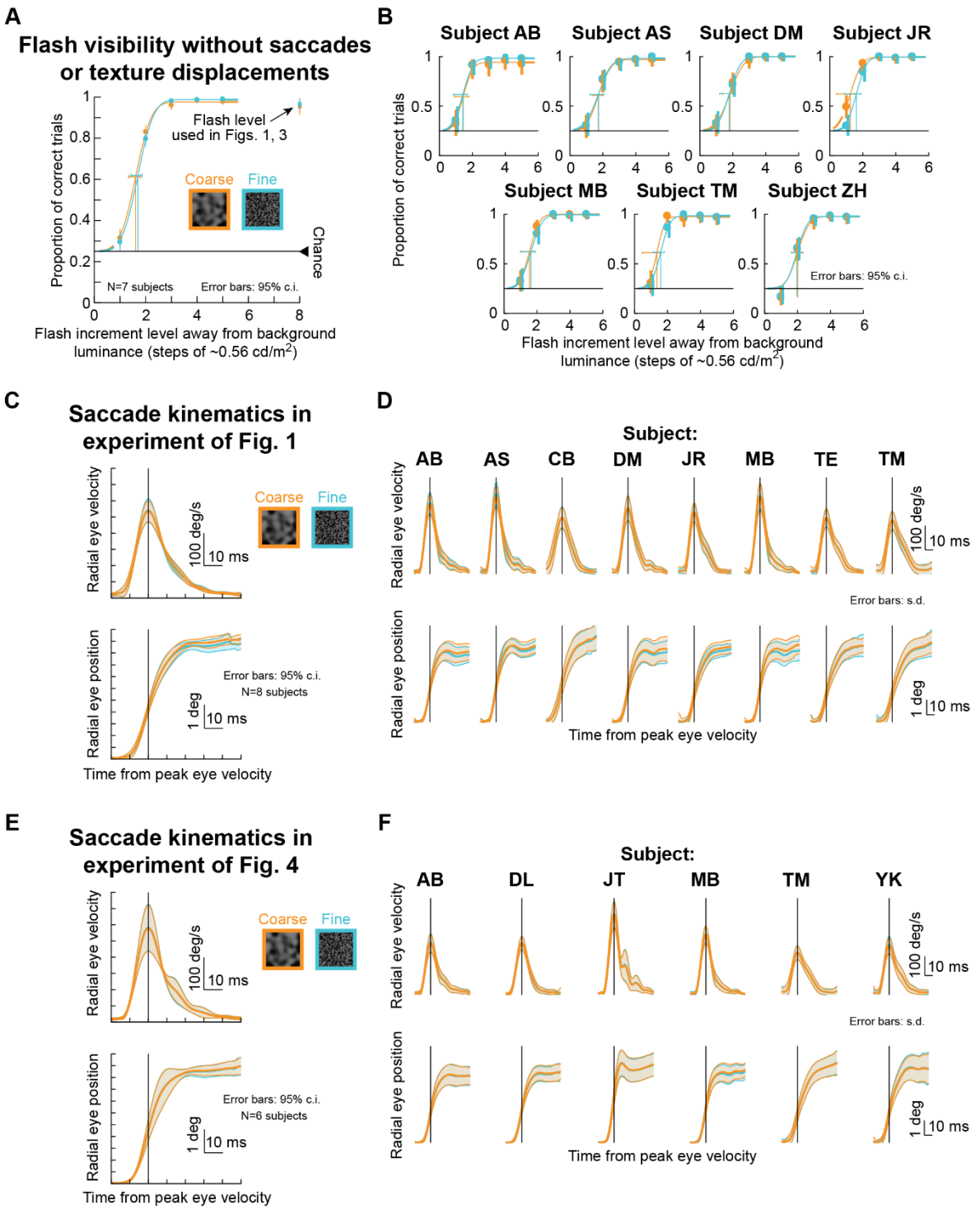

Fig. S3 Controls for flash visibility and motor variability in our perceptual experiments. (A) For the same textures as in Figs. 1, 3, we asked subjects to maintain fixation, and we eliminated both real saccades (Fig. 1) as well as saccade-like texture displacements (Fig. 3). At a random time during fixation, a luminance pedestal appeared exactly as in the main experiments, but this time, we varied its contrast from background across trials (Methods). We ensured that no microsaccades occurred near the time of flash onset (Methods). Psychometric curves of localization performance indicate that, at the flash contrast used in Figs. 1, 3 (highlighted by the black arrow), subjects could easily detect flashes during fixation and without visual transients associated with saccade-like texture displacements. Importantly, flash visibility was identical for coarse or fine textures at all flash contrasts. Therefore, flash

visibility alone (or lack thereof) did not explain the main experiments' results (Figs. 1, 3), including differences in perception caused by coarse and fine textures. The strong suppression observed in Figs. 1, 3 was instead likely a function of interaction between visual transients associated with saccades or texture displacements and the flashes. **(B)** This idea is further supported by the fact that all individual subjects that performed the present control experiment showed consistent results. All of these subjects had also participated in the experiments of Figs. 1, 3 (with the exception of subject ZH who only performed the control experiment). Psychometric curves were fit using the *psignifit 4 toolbox* (Schütt *et al.*, 2016), and error bars denote 95% confidence intervals. **(C)** We also checked for potential effects of motor variability on perceptual performance, in order to rule out the possibility that differences in performance between textures (Fig. 1) were due to differences in eye movement kinematics. For the experiments of Fig. 1, we plotted average radial eye velocity (top) and average radial eye position (bottom) across subjects (error bars denote 95% confidence intervals across the individual subjects' curves). There was no effect of background texture on eye movement kinematics. **(D)** This was also true for each individual subject. In this case, error bars denote s.d. across trials, further supporting that saccade kinematics were not different when saccades were made across coarse or fine textures. **(E, F)** Same kinematic analyses, but now for the saccades of the experiment of Fig. 4.

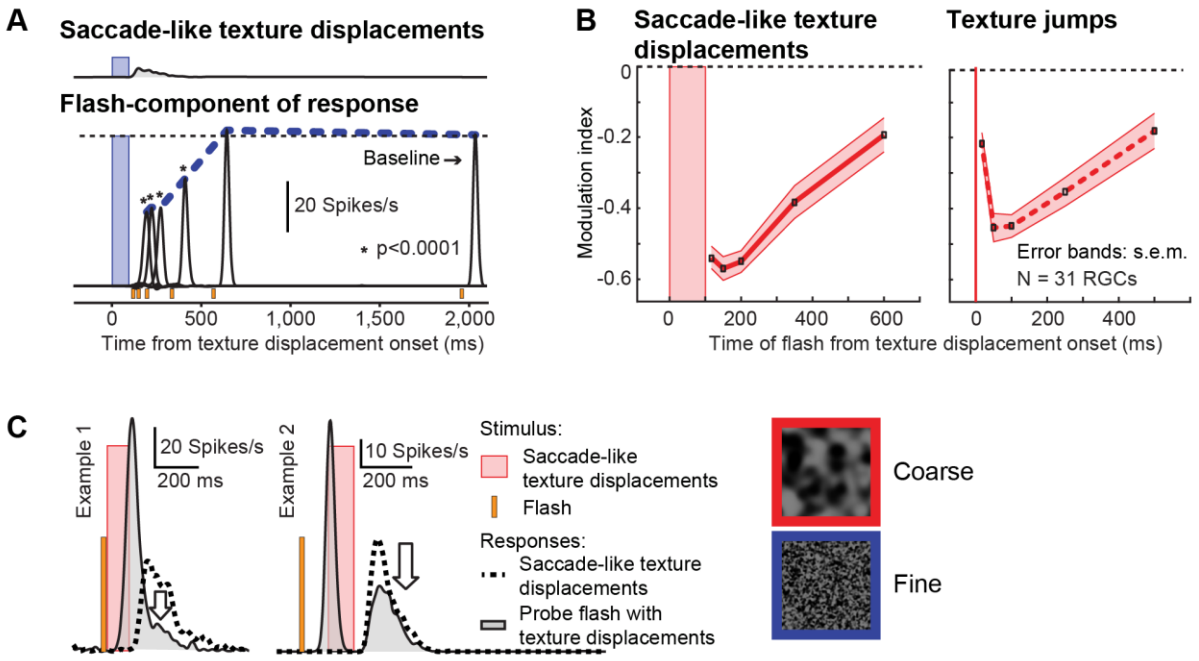

Fig. S4 Properties of retinal "saccadic suppression". (A) Example RGC that responded only weakly to texture displacements (top), but nevertheless still exhibited strong suppression of flash-induced neural responses (bottom; both curves are plotted at the same scale). The suppression was much stronger than the response amplitude to the texture displacement alone; therefore, suppression was not a result of neural activity saturation due to successive visual stimulation of the cell (first by the texture displacement and then by the flash). **(B)** Retinal suppression also did not depend on the velocity properties of texture displacement. We observed very similar suppression of flash-induced neural responses when the texture jumped from the pre- to post-displacement positions in one display frame (right) compared to our standard paradigm, in which the same texture displacement occurred over 100 ms in 6 equal successive steps (left). This means that retinal "saccadic suppression" was mainly governed by stimulus-stimulus interactions, with the first stimulus influencing the responses to the second. **(C)** Examples of two RGCs for which we presented a flash before the saccade-like texture displacement. The response to the second stimulus (texture displacement) was suppressed because of the first stimulus (flash), supporting the notion that stimulus-stimulus interactions are the main drive for retinal "saccadic suppression".

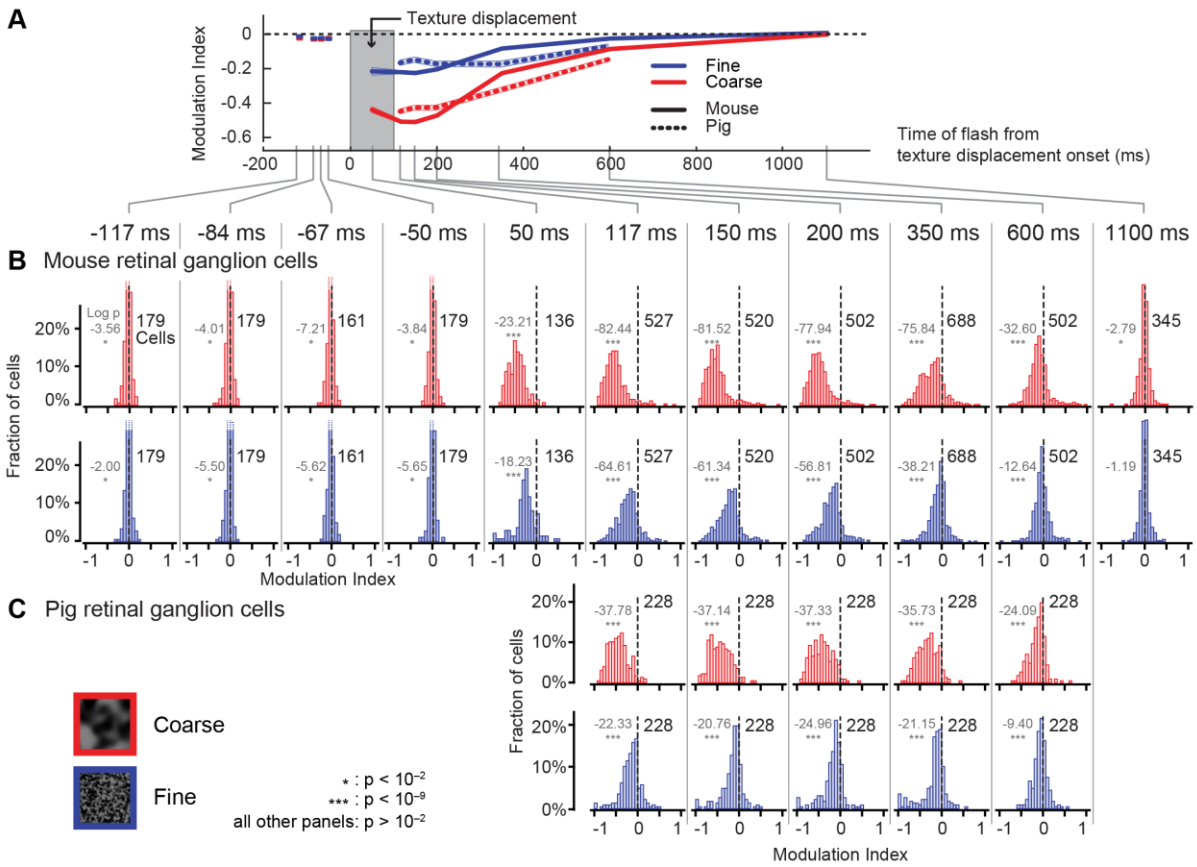

Fig. S5 Population data detailing the properties of retinal "saccadic suppression". (A) Replication of Fig. 2E, showing the time courses of retinal "saccadic suppression" in mouse and pig retinae. **(B, C)** Histograms of neuronal modulation indices for mouse **(B)** and pig **(C)** RGCs at different flash times relative to texture displacement onset. Red and blue denote coarse and fine textures, respectively. Black numbers in each panel indicate the numbers of RGCs analyzed for each condition; gray numbers show the logarithm (base 10) of the exact p-value (two-tailed Wilcoxon signed-rank test to determine if the population median was shifted away from 0). Asterisks additionally indicate the level of significance.

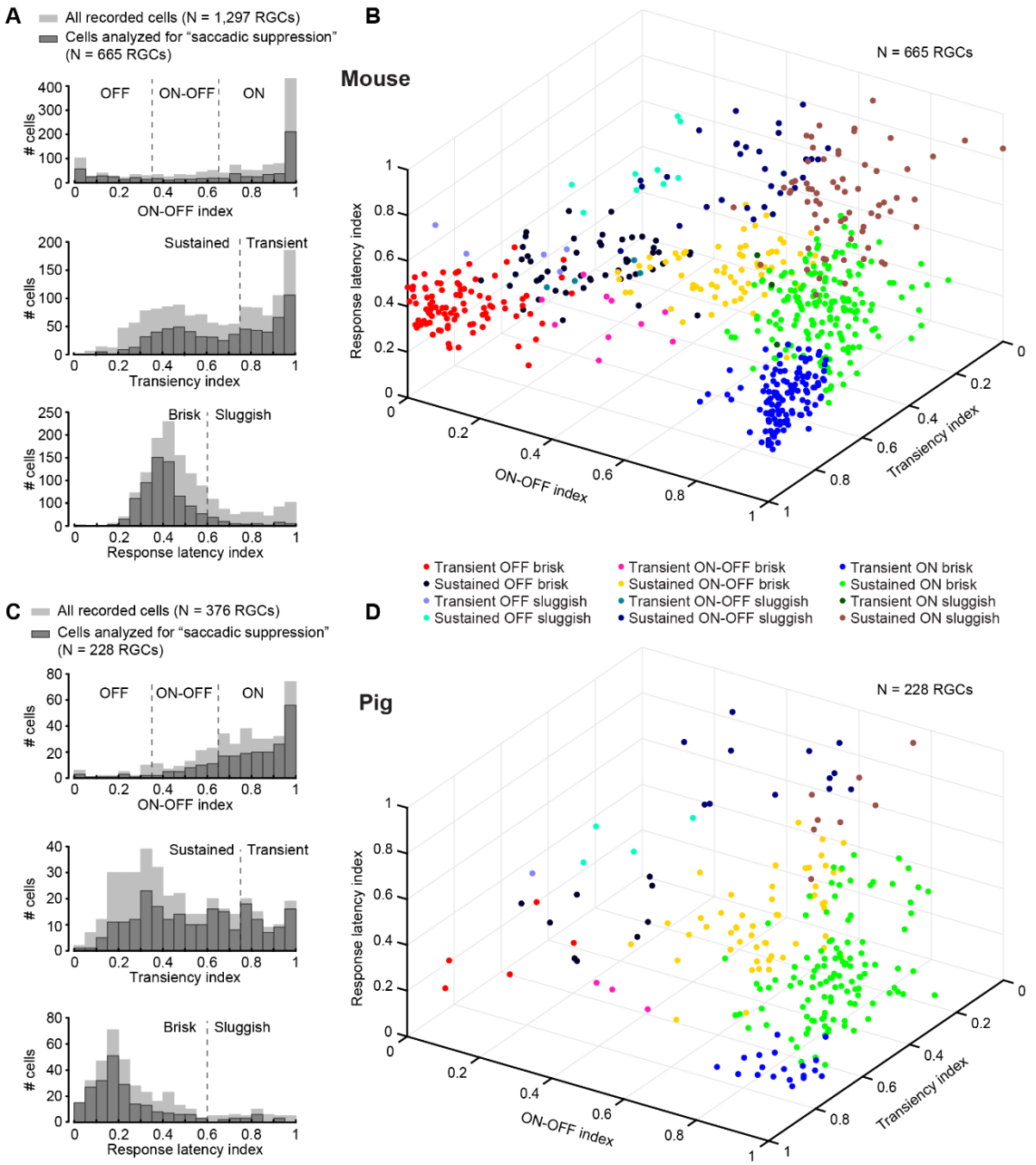

Fig. S6. Diverse properties of RGCs included in our analysis. We quantified the response properties of all recorded mouse **(A, B)** and pig **(C, D)** RGCs with respect to three neuronal response properties (see Methods): ON-OFF index, transiency index and response latency index. Each histogram **(A, C)** was divided into 2 or 3 groups: RGCs could be OFF, ON-OFF, or ON (top histograms); transient or sustained (middle histograms); and brisk (short response latency) or sluggish (long response latency) (bottom histograms). Combined, this resulted in 12 response categories to which each recorded RGC belonged. The cells that could be analyzed for "saccadic suppression" and for which the response properties could be computed (dark gray histograms) spanned the entire range of response indices exhibited by all recorded cells for which these response properties were analyzed (light gray histograms). The three-dimensional scatter plots **(B, D)** show the projection of the RGC subsets considered in our analysis for "saccadic suppression" onto the 3 neuronal response indices. The 12 response categories, formed by the combination of histograms in **(A, C)**, can be seen in different colors.

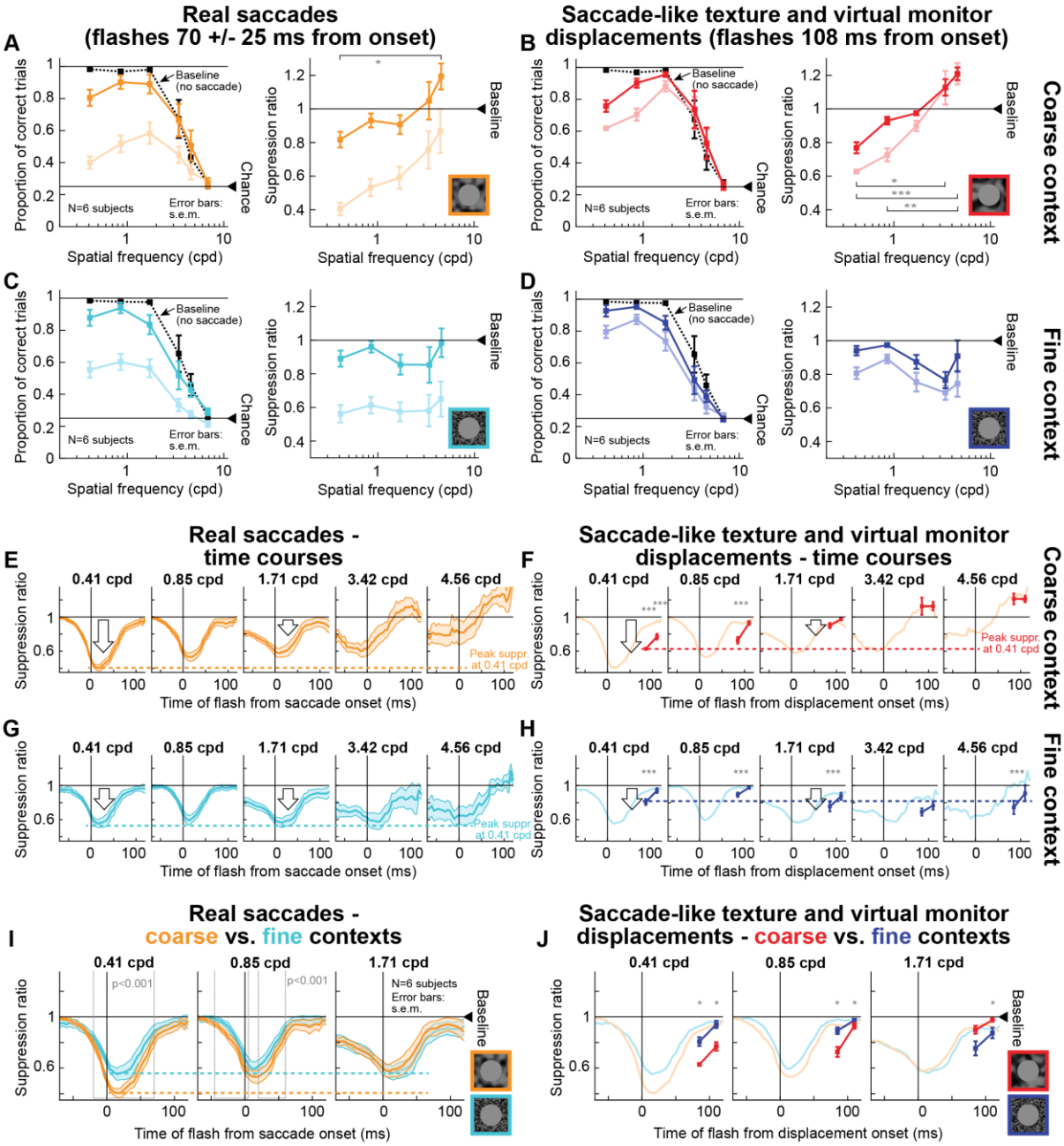

Fig. S7. Time courses of perceptual suppression with real and "simulated" saccades in the experiment of Fig. 4. (A) Same analysis as in Fig. 4B, but at a later time point of grating flash onsets relative to saccade onset. Faint curves show the data from Fig. 4B for comparison (the baseline curves apply to both time points since they were collected without any saccades). At around 70 ms after saccade onset, perceptual recovery from saccadic suppression emerged, but the selectivity of suppression across different spatial frequencies was still present (there was a main effect of spatial frequency on suppression ratio; χ^2=11.4, p=0.022, df=4, Kruskal-Wallis test). All other conventions are as in Fig. 4B (* p<0.05, post-hoc pairwise test between the lowest and highest spatial frequencies). **(B)** Same analysis as in Fig. 4D, but at a later time point of flash onset after virtual monitor and texture displacement. The same observations as in **A** were made: perceptual recovery occurred at the later time point, but selectivity of suppression was still obvious (χ^2=25.26, p<0.0001, df=4, Kruskal-Wallis test, same post hoc conventions as in Fig. 4D). The faint curves show the data from Fig. 4D for comparison. Note how this condition of displacements of the virtual monitor and texture surround resulted in longer lasting suppression than with real saccades (also see **E-H**). **(C, D)** Same analyses as in

A and **B**, but with a fine texture surrounding the virtual monitor (Fig. 4E, F). **(E)** Time courses of suppression from Fig. 4A, B with a coarse surround around the virtual monitor. We used similar binning procedures to Fig. 1. Peak suppression was strongest when 0.41 cpd gratings were flashed and progressively weakened for higher spatial frequency gratings (horizontal colored dashed line across panels). **(F)** With simulated saccade-like virtual monitor and texture displacements, we sampled two grating flash times relative to displacement onset. Recovery at the later time point for each grating spatial frequency was evident. Moreover, selectivity of suppression as a function of grating spatial frequency was evident (horizontal colored dashed line across panels demonstrating the peak suppression for the lowest spatial frequency). The faint curves show time courses from **e** for comparison. Note how simulated saccades caused longer-lasting suppression than real saccades, exactly as in the experiment of Fig. 3 (*** $p<0.0001$, χ^2 tests with Bonferroni corrections comparing perceptual suppression with the simulated condition to a corresponding time bin in the real condition). **(G, H)** Similar analyses for fine texture surrounds around the virtual monitor. In this case, suppression was the same across all spatial frequencies (horizontal colored dashed lines across panels). **(I)** For real saccades, and for low spatial frequencies of gratings (i.e. when both coarse and fine surround contexts were associated with strong saccadic suppression), the coarse surround was associated with longer lasting suppression than the fine surround. This is consistent with the results of Fig. 1 when saccades were generated across full-screen textures. **(J)** This texture-dependence was also true with "simulated" saccades (* $p<0.05$, random permutation test comparing coarse and fine textures at a given grating flash time). Error bars in all panels denote s.e.m. All other conventions are as in Figs. 1, 3, 4.

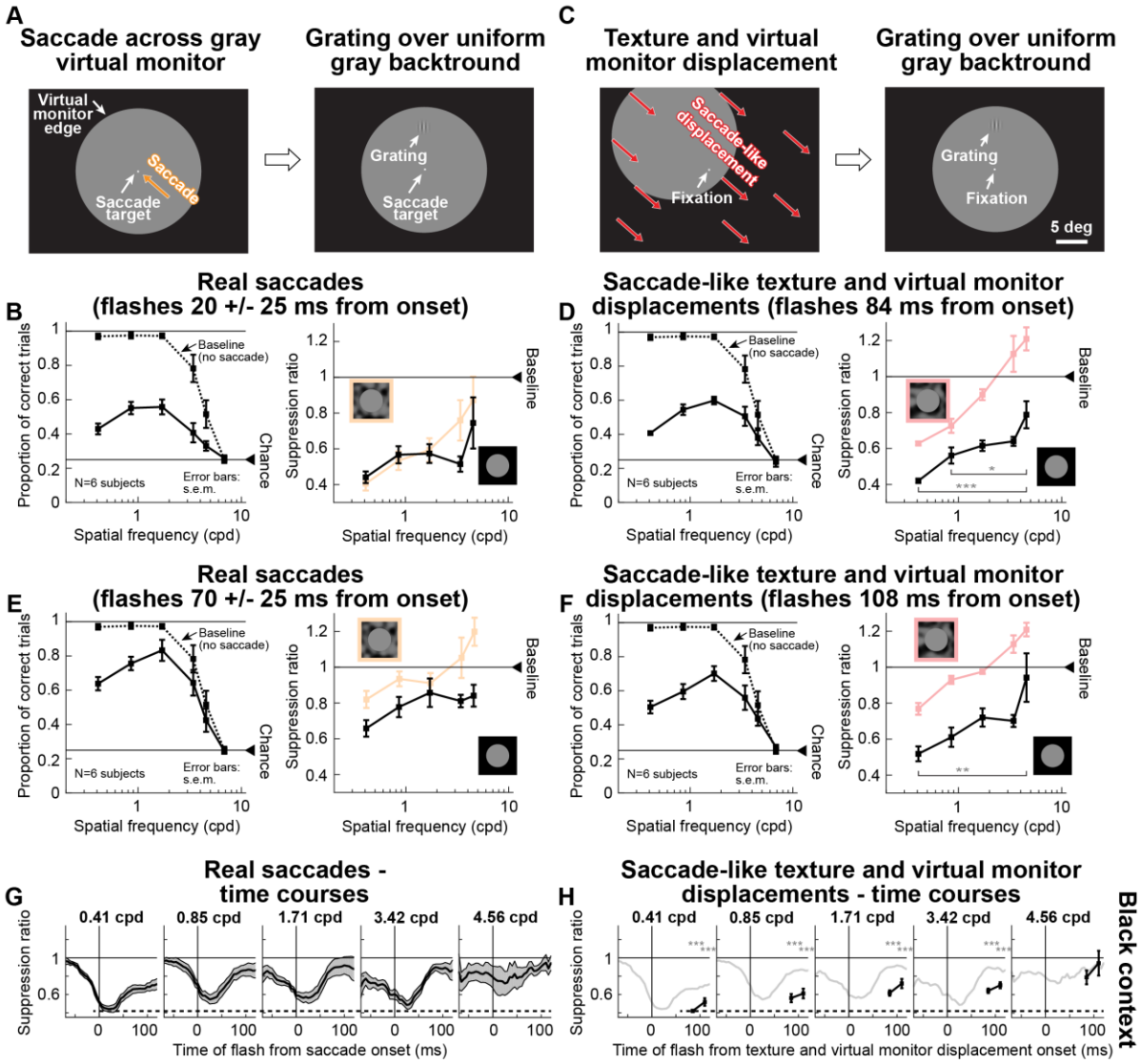

Fig. S8. Replicating the results of Fig. 4 but with black surrounds around a uniform gray display. (A) We repeated the same experiment as in Fig. 4A but this time using a black surround around the virtual monitor, as one might normally do in experiments on saccadic suppression (Hafed and Krauzlis, 2010; Chen and Hafed, 2017). Note that a black (or white) surround is theoretically equivalent to an infinitely coarse surround; hence, we expected observations more similar to Fig. 4A-D (i.e. selectivity of suppression for low spatial frequencies) than Fig. 4E, F. **(B)** Similar suppression selectivity for low spatial frequencies occurred with real saccades as in Fig. 4B (faint curves replicate that data for comparison). **(C)** Same experiment as in Fig. 4C, but with a black surround. **(D)** Selectivity of suppression for low spatial frequencies was even more evident with "simulated" saccades. Faint curves show results from Fig. 4D for comparison. **(E, F)** Similar analyses at a later time point, identical to Fig. S7A-D. There was recovery for both real (**E**) and simulated (**F**) saccades (faint colored curves show data from Fig. S7A, B at the same time points for easier comparison). Note that with black surrounds, suppression strength was larger overall than with either coarse or fine texture surrounds (as if the black surround was indeed an extension of the coarseness of the texture). **(G, H)** Full time courses of suppression as in Fig. S7. All error bars denote s.e.m., and all conventions are similar to Fig. 4 and Fig. S7.

Methods

Ethical approvals

We performed electrophysiological experiments on ex vivo mouse and pig retinae as well as non-invasive perceptual experiments on human subjects.

Animal use was in accordance with German and European regulations, and animal experiments were approved by the Regierungspräsidium Tübingen.

Human subjects provided written, informed consent, and they were paid 8 Euros per session of 45-60 minutes each. Depending on the experiment, each subject was measured for 2-10 sessions (detailed trial and session numbers are provided below). Human experiments were approved by ethics committees at the Medical Faculty of Tübingen University, and they were in accordance with the Declaration of Helsinki.

Data availability

All data are stored and archived on secure institute computers, and they are available upon reasonable request.

Retina electrophysiology laboratory setup

We used retinae extracted from PV-Cre x Thy-S-Y mice (B6;129P2-Pvalb$^{tm1(cre)Arbr}$/J × C57BL/6-tg (ThystopYFPJS), which are functionally wild type (Münch *et al.*, 2009; Farrow *et al.*, 2013; Tikidji-Hamburyan *et al.*, 2015). 19 retinae from 6 male and 12 female mice (3-12 months old) were used. We also replicated experiments on pig retinae obtained from domestic pigs after they had been sacrificed during independent studies at the Department of Experimental Surgery in our Medical Faculty. We used 9 pig retinae.

We housed mice on a 12/12 h light/dark cycle, and we dark adapted them for 4-16 h before experiments. We then sacrificed them under dim red light, removed the eyecups, and put them in Ringer solution (in mM: 110 NaCl, 2.5 KCl, 1 $CaCl_2$, 1.6 $MgCl_2$, 10 D-glucose, and 22 $NaHCO_3$) bubbled with 5% CO_2 and 95% O_2. We removed retina from the pigment epithelium and sclera while in Ringer solution.

Pigs were anesthetized using atropine, azaperone, benzodiazepine (midazolam), and ketamine, and then sacrificed with embutramide (T61). Before embutramide administration, heparin was injected. The pigs were dark-adapted for 15-20 min before sacrifice. Immediately after sacrifice, the eyes were enucleated under dim red light, and the cornea, lens, and vitreous were removed. Eyecups were kept in CO_2-independent culture medium (Gibco) and protected from

light. We transported eyecups to our laboratory and cut pieces from mid-peripheral or peripheral retinae.

We recorded retina ganglion cell (RGC) activity using either low or high-density multi-electrode arrays (MEAs). The low-density setup consisted of a perforated 60-electrode MEA (60pMEA200/30ir-Ti-gt, Multichannel Systems, Reutlingen, Germany) having a square grid arrangement and 200 μm inter-electrode distance. We mounted an isolated retina on a nitrocellulose filter (Millipore) with a central 2x2 mm hole. The mounted retina was placed with the RGC side down into the recording chamber, and good electrode contact was achieved by negative pressure through the MEA perforation. We superfused the tissue with Ringer solution at 30-34 °C during recordings, and we recorded extracellular activity at 25 kHz using a USB-MEA-system (USB-MEA 1060, Multichannel Systems) or a memory-card based system (MEA1060, Multichannel Systems). More details are provided in (Reinhard *et al.*, 2014).

The high-density MEA setup consisted of either a HiDens CMOS MEA (Frey *et al.*, 2009) or a MaxOne system (Müller *et al.*, 2015). The HiDens CMOS MEA featured 11,011 metal electrodes with inter-electrode (center-to-center) spacing of 18 μm placed in a honeycomb pattern over an area of 2 x 1.75 mm. For simultaneous recording, any combination of 126 electrodes could be selected. The MaxOne MEA featured 26,400 metal electrodes with center-to-center spacing of 17.5 μm over an area of 3.85 x 2.1 mm. In this system, up to 1,024 electrodes could be arbitrarily selected for simultaneous recordings. For each experiment, a piece of isolated retina covering almost the entire electrode array was cut and placed RGC side down in the recording chamber. We achieved good electrode contact by applying pressure on the photoreceptor side of the retina by carefully lowering a permeable membrane with the aid of a micromanipulator. We recorded extracellular activity at 20 kHz using FPGA signal processing hardware and custom data acquisition software.

In total, we performed 32 recordings, 20 from mouse and 12 from pig retina. 15 of the 32 recordings were done using low-density MEAs. Once a basic experimental protocol was established, we shifted to HiDens CMOS MEA providing much higher throughput. 12 experiments were done using this setup. We upgraded to the MaxOne MEA for even higher throughput and did our final 5 recordings using this setup.

We presented light stimuli to the retinal piece that was placed on the MEA using a DLP projector running at 60 Hz (Acer K11 for low-density MEA experiments and Lightcrafter 4500 for high-density MEA experiments). Acer K11 had a resolution of 800x600 pixels

covering 3 x 2.25 mm on the retinal surface. Lightcrafter 4500 had a resolution of 1280x800 pixels, extending 3.072 x 1.92 mm on the retinal surface. We focused images onto the photoreceptors using a condenser. The light path contained a shutter and two motorized filter wheels with a set of neutral density (ND) filters (Thorlabs NE10B-A to NE50B-A), having optical densities from 1 (ND1) to 5 (ND5). Light intensity was adjusted to be in the mesopic range.

We measured the spectral intensity profile (in µW cm^{-2} nm^{-1}) of our light stimuli with a calibrated USB2000+ spectrophotometer (Ocean Optics) and converted the physical intensity into a biological equivalent of photoisomerizations per rod photoreceptor per second ($R^*rod^{-1}s^{-1}$), as described before (Tikidji-Hamburyan *et al.*, 2015). Light intensities of the projector output covered a range of 3 log units (i.e. 1,000-fold difference between black and white pixels, over an 8-bit range). We linearized the projector output, and we used only grayscale images of limited contrast, spanning at most the range from 0 to 120 in the 8-bit range of the projector (see stimulus description below for details). Absolute light intensities were set to the mesopic level, where a stimulus intensity of '30' in our 8-bit DLP projector scale (0-255) corresponded to 225 to 425 $R^*rod^{-1}s^{-1}$, depending on the experimental rig used for the experiment (i.e. different DLP projectors and MEAs). We pooled all data from the different rigs because separate individual analyses from the individual setups revealed no effects of recording conditions in the different setups.

Human psychophysics laboratory setup

We used a similar laboratory setup to (Hafed, 2013; Bellet, Chen and Hafed, 2017; Grujic *et al.*, 2018). Briefly, subjects sat in a dark room 57 cm in front of a CRT monitor (85 Hz refresh rate; 41 pixels/deg resolution) spanning 34.1 x 25.6 deg (horizontal x vertical). Head fixation was achieved with a custom head, forehead, and chin rest (Hafed, 2013), and we tracked eye movements (of the left eye) at 1 kHz using a video-based eye tracker (EyeLink 1000, SR Research Ltd, Canada). Gray and texture backgrounds (e.g. Figs. 1, 3, 4) were always presented at an average luminance of 22.15 cd/m^2, and the monitor was linearized (8-bit resolution) such that equal luminance increments and decrements were possible around this average for textures and gratings.

Human Experiment 1 (Fig. 1) was performed by 8 subjects (2 female) who were 21-25 years old. All subjects were naïve to the purposes of the experiment, except for subject MB (an author). For Human Experiment 2, the "simulated saccade" version of Human Experiment 1 (Fig. 3), 6 of the same subjects participated. A control experiment for testing visibility of

flashes without saccades and without saccade-like texture displacements (e.g. Fig. S3A, B) was performed by 6 of the same subjects plus one non-naïve subject, ZH (another author).

Human Experiment 3 tested suppression selectivity for low spatial frequencies (Fig. 4). Six subjects (3 females, 23-25 years old) participated, and only subject MB was non-naïve. Three subjects had also participated in Human Experiments 1 and 2 and their control version. A control version of Human Experiment 3 was also performed with black surrounds (Fig. S8). This control experiment was performed by the same subjects that participated in Human Experiment 3.

Across all experiments, we ensured that the same subjects performed real and "simulated" saccade versions of a given paradigm so that we could make meaningful comparisons between these two eye movement conditions.

Coarse and fine textures used in retina electrophysiology and human psychophysics experiments

We created coarse and fine textures (Fig. S1A) by convolving a random binary (i.e. white or black) pixel image with a two-dimensional Gaussian blurring filter (Schwartz *et al.*, 2012) with the kernel

$$G(x,y) = e^{\frac{-(x^2+y^2)}{2\sigma^2}}$$

The parameter σ of the kernel influenced the amount of blurring. This resulted in textures having effectively low-pass spectral content (Fig. S1B) with a cutoff frequency (f_c) depending on σ. As we describe below, we picked cutoff frequencies for coarse and fine textures that resulted in dark and bright image blobs approximating the receptive field sizes of RGCs (for coarse textures) and retinal bipolar cells (for fine textures). In other words, for a given species, coarse textures matched the resolution of RGCs, and fine textures matched the resolution of one processing stage earlier, the retinal bipolar cells.

For the ex-vivo experiments with mouse and pig retinae, we assumed receptive field diameters for RGCs of at least 150 µm (Fig. S1C; the parameter σ of the Gaussian blurring filter would be half that value), and diameters for bipolar cells of 25 µm (see (Zhang *et al.*, 2012)). For human psychophysics experiments, we estimated, from the literature (Dacey and Petersen, 1992), the sizes of human parasol RGC receptive fields at eccentricities >6 deg from the fovea (our flash eccentricities were 7 deg) to be around 200 µm. This translated into a cutoff frequency of ~0.68 cycles per deg (cpd) (Fig. S1B). Bipolar cell receptive field sizes at this eccentricity were estimated to be 10 µm (corresponding to a cutoff frequency of ~13.7 cpd), based on sizes of human midget RGC receptive fields in the fovea (Dacey and Petersen,

1992). When calculating the textures, the actual value of the parameter σ (in pixel-dimensions) always incorporated the specific experimental magnification factor between the stimulation screen and the retinal projection of the image.

Calculating power spectra for coarse and fine textures confirmed that cutoff frequencies for a given species were consistent with our aimed designs described above (Fig. S1B).

For both retinal and perceptual experiments, we normalized pixel intensities in the textures to have uniform variations in luminance around a given mean. In the retinal experiments, we used pixel intensities (from our 8-bit resolution scale) ranging from 0 to 60 around a mean of 30, or ranging from 30 to 90 around a mean of 60 (see flash conditions below for when each paradigm was used). For the human experiments, textures had a mean luminance of 22.15 cd/m^2 with undulations in luminance in the texture within the range of 7.5-35.5 cd/m^2.

Because each texture, particularly when coarse, could have patterns of dark and bright blobs that human subjects can remember or interpret as potential shapes/objects/figures, we varied the displayed texture images from trial to trial. This was also necessary to avoid afterimages. We generated sets of 20 coarse and 20 fine textures, which we randomly interleaved across trials. Moreover, the textures themselves were designed to be larger than the viewable display area, allowing us to jitter the displayed sub-rectangle of each texture (within the viewable area of the display) from trial to trial (we jittered the displayed sub-rectangle within a range of 0.6 x 0.6 deg in steps of 0.024 deg). This way, even fine patterns at foveal fixation locations could not be memorized by the subjects.

Retina electrophysiology experimental procedures

To simulate saccades in our ex vivo retina electrophysiology experiments, we displaced the texture across retina in 6 display frames (100 ms at 60 Hz refresh rate). For easier readability, we sometimes refer to these saccade-like texture displacements as “saccades”. The textures were displaced in each frame by a constant distance along a linear trajectory. While each “saccade” lasted 100 ms, displacement direction was varied randomly for each “saccade” (uniformly distributed across all possible directions) and “saccade” amplitude could range from 310 μm to 930 μm (corresponding to a velocity range of 3,100-9,300 μm/s on the retinal surface). In visual degrees, this displacement corresponds to 10-30 deg, well in the range of saccade amplitudes observed in mice (Sakatani and Isa, 2007) and velocities of 100-300 deg/s and 10-32 deg/s for mouse and pig eyeball sizes, respectively.

Each “trial” consisted of 39 successive sequences that each combined a “saccade” with a probe flash, as follows: there was first a “pre-saccade” fixation of 2 seconds, then a 100 ms

"saccade", followed by "post-saccade" fixation. At a certain time from "saccade" onset (delay d, range: -177 ms to 2,100 ms), we presented a probe flash. In most cases, the probe flash had a duration of 1 frame (~16 ms), we used 2 frames (~33 ms) in a subset of experiments (mouse: 161/688 cells analyzed for "saccadic suppression"; pig: 112/228 cells). Results were pooled across these paradigms as they were indistinguishable. For sequences containing no probe flash, the next "saccade" happened 4 s after the previous one. The probe flash was a full-screen positive ("bright") or negative ("dark") stimulus transient. In different experiments, only a subset of possible delays was used within a given set of trials, depending on total recording time for a given retina (see below).

Bright or dark probe flashes could happen in two different ways across our experiments. The results were indistinguishable between the two ways, so we pooled results across them. Briefly, in one manipulation, the probe flash was a homogeneous bright (pixel intensity of 60 in our 8-bit projectors) or dark (pixel intensity of 0) full-screen rectangle replacing the background texture (in these experiments, the textures themselves had intensities ranging from 0 to 60 pixel intensity; see coarse and fine texture descriptions above). This way, the flash contrast from the underlying background luminance was variable (e.g. a bright flash on a bright portion of a texture had lower contrast from the underlying texture than the same flash over a dark portion of the texture). In the second manipulation, the bright and dark flashes were simply luminance increments or decrements (by pixel values of 30 on our 8-bit projectors) over the existing textures (like in our human perceptual experiments). This way, local contrast relationships in the background textures were maintained. In these experiments, the textures themselves had a range of 30-90 pixel intensities and a mean pixel value of 60 (on our 8-bit projectors). 332/688 cells we analyzed for "saccadic suppression" experienced such probe flashes whereas the rest (356 cells) experienced the homogenous probe flash. For pig retina recordings, we always used the homogenous framework. However, in the subset of pig experiments where the 2-frame probe flash was employed (112/228 RGCs), we used a high-contrast probe flash such that a bright flash would be achieved by first going completely dark in the first frame followed by the bright flash in the next frame and vice versa for a dark flash. Again, all data was pooled across these different paradigms because their outcome was indistinguishable.

The number of trials required during a physiology experiment depended on the number of conditions that we ran on a specific day. For example, testing 7 different flash delays required 15 trials (7 with bright probe flashes, 7 with dark probe flashes, and 1 without probes). In a given experiment, we always interleaved all conditions; i.e. in any one of the 15 necessary

trials, each of the 39 “saccades” could be followed by a bright or a dark probe at any of the 7 delays, or no probe at all. Moreover, we repeated the total number of conditions (e.g. the interleaved 15 trials) 4 times per session, and we averaged responses across repetitions. Since one trial typically lasted for 2 minutes, the example of 15 trials repeated 4 times lasted for approximately 2 hours. This was usually combined with additional conditions (e.g. other background textures), such that typical recordings lasted 10-12 hours. If the combination of conditions would have required even longer recordings in a given session, we typically reduced the number of conditions (e.g. we presented flashes at fewer delays).

We sometimes replaced the 100 ms “saccade” with an instantaneous texture jump, to test the sensitivity of retinal “saccadic suppression” (Fig. 2) to the properties of saccade-like texture displacements (Fig. S4B). Here the texture simply jumped, in one display frame, from the pre- to the post-displacement position. All other procedures were like described above.

Finally, we used other stimuli to help us characterize RGC types and other receptive field properties (e.g. response polarity, latency, transiency, and spatial receptive fields). These stimuli had the same mean intensities and intensity ranges as the textures used in each experiment. Below, we describe these stimuli for the condition in which the texture intensities ranged from 0 to 60 pixel intensity (represented as grayscale RGB values in the units of our 8-bit projects). In experiments in which the textures ranged in intensity from 30 to 90, all intensities reported below were shifted upward by 30. (1) Full-field contrast steps. ON steps: stepping from 0 to 30 (+1 Michelson contrast) and from 30 to 60 (+0.33) for 2s. OFF steps: stepping from 60 to 30 (-0.33) and from 30 to 0 (-1) for 2s. (2) Full-field Gaussian flicker, 1min. Screen brightness was updated every frame and was drawn from a Gaussian distribution with mean 30 and s.d. 9. This stimulus was used to calculate the linear filters of ganglion cells through reverse correlation (spike-triggered averaging of the stimulus history). (3) Binary checkerboard flicker, 10-15 min. The screen was divided into a checkerboard pattern; each checker either covered an area of 55 x 55 µm, 60 x 60 µm, or 65 x 65 µm depending on the configuration. The intensity of each checker was updated independently from the other checkers and randomly switched between 10 and 50 or 0 and 120. This stimulus also allowed us to calculate the linear filters of cells’ receptive fields.

Human psychophysics experimental procedures

In Human Experiment 1, we presented a coarse or fine background texture (Fig. 1) for 800-1,700 ms in every trial. Over the texture, a white fixation marker (square of 7.3 x 7.3 arcmin) surrounded by a uniform gray circle of 30 min arc radius was presented at one screen location

in order to guide gaze fixation onto the marker. The fixation marker was always at 4.8 deg eccentricity from display center, but its specific location was varied from trial to trial (up-right, up-left, down-right, or down-left relative to display center; 45 deg direction from horizontal). After the end of the initial interval, the fixation marker jumped to display center, instructing subjects to generate a saccade.

At a random time from the saccade instruction (47, 94, 153, 200, 247, or 507 ms), a luminance pedestal (probe flash) was applied for one display frame (~12 ms) at one of four locations relative to display center (7 deg above, below, to the right of, or to the left of center). The pedestal consisted of a square of 147.8 x 147.8 min arc in which we added or subtracted a value of 4.8 cd/m^2 to the texture pattern. Therefore, local contrast within the luminance pedestal was the same as that without the pedestal. Since all of our analyses revealed identical results whether the pedestal was a luminance increment or decrement, we combined these conditions in all analyses. At the end of the trial, subjects had to report their perceived flash location by pressing one of four buttons, corresponding to the four possible flash locations, on a hand-held response box.

Because saccadic reaction times were 156.9 +/- 3.3 ms s.e.m. across subjects, our choice of flash times above meant that we could analyze trials in which flashes appeared before or after saccade onset, allowing us to obtain full time courses (e.g. Fig. 1). Also, because of the display geometry, the retinal region that experienced a flash before, during, or after a saccade was always a region that was visually-stimulated by the texture before flash onset (rather than by the monitor edge or the black surround of the laboratory). Therefore, we maintained pre- and post-flash visual stimulation by texture background, as in the retinal experiments. We also ensured that flash locations were not coincident with saccade goal locations both retinotopically and also in display coordinates. We confirmed in separate analyses that similar effects of suppression (e.g. Fig. 1) occurred for each flash location separately (data not shown).

We collected 576 trials per session in this experiment. Six subjects participated in 6 sessions each, and the remaining two participated in 3 or 4 sessions.

Human Experiment 2 was identical, except that the initial fixation marker was presented at display center and remained there for the entire duration of a trial. Instead of instructing a saccade 800-1,700 ms after fixation marker onset, we translated the entire background texture rapidly to simulate a saccade-like image displacement. Texture displacement consisted of a 6-frame translation at a speed of 176 deg/s. Note that, because of our display refresh rate and

geometry, this meant a slightly larger displacement (of 12.4 deg) when compared to the saccade sizes in Human Experiment 1. However, we chose this translation because it resulted in a sufficiently fast average speed of the displacement (average speed in the real saccades of Human Experiment 1 was 160 deg/s). This choice is not problematic because our retinal experiments revealed that visual mechanisms related to saccadic suppression were not sensitive to parameters of individual motion patterns (Fig. S4B).

In this experiment, the texture displacement happened in a diagonal direction to simulate the directions of saccadic displacements of Human Experiment 1 (and also to dissociate the direction of motion flow from the locations of the flashes, again as in Human Experiment 1). For example, the texture could move globally down-right, as might be expected (in terms of image motion) if subjects made upward-leftward saccades in Human Experiment 1. Also, flash times were chosen relative to the onset of texture displacement (from among the following values: -35, -24, 24, 47, 84, 108, 141, 200, 259, 494 ms).

All subjects participated in 10 session each in this experiment.

We also performed a control experiment, in which there was neither a real saccade (Human Experiment 1) nor a texture displacement (Human Experiment 2), but otherwise identical to these 2 experiments. Subjects simply fixated display center, and we presented (after 1,200 to 2,400 ms from trial onset) a luminance pedestal exactly as in Human Experiments 1 and 2. To obtain full psychometric curves, we varied the luminance increment from among 6 values (e.g. Fig. S3A, B). Subjects performed two sessions each of this experiment (600 trials per session).

In Human Experiment 3 (Fig. 4), the flashes of Human Experiments 1 and 2 were replaced by vertical Gabor gratings having one of five different spatial frequencies (0.41, 0.85, 1.71, 3.42, 4.56, or 6.8 cpd). Spatial phase was randomized from trial to trial, and the σ parameter of the Gaussian envelope was 0.49 deg. Also, a virtual monitor of 20 deg diameter was present at display center at the time of grating flashes. The virtual monitor had a uniform gray luminance equal to the average of the textures used in Human Experiments 1 and 2. Surrounding the virtual monitor, a coarse or fine texture could be visible.

In one block of trials, subjects generated saccades towards display center using the same procedures as in Human Experiment 1. Grating flash times were similar to Human Experiment 1, and the subjects performed 6 sessions each (576 trials per session).

In another block of trials, subjects maintained fixation at display center. In one third of the trials, the virtual monitor and surrounding texture did not move. These trials provided us with

"baseline" visual performance (i.e. without saccades or virtual monitor displacements). It was necessary to have these trials because perceptual visibility of different spatial frequencies is not equal due to the well-known human contrast sensitivity function (Peli *et al.*, 1993). Therefore, we needed to establish "baseline" grating visibility first and then compare the effects of saccades or saccade-like virtual monitor displacements on such visibility. In the remaining two thirds of the trials, the virtual monitor and surrounding texture initially appeared displaced from display center at a location near one corner of the display and along one of the diagonal directions. After 800-1,700 ms, the virtual monitor and surrounding texture were translated rapidly towards display center to simulate visual flow associated with the diagonal saccades of the real-saccade version of the paradigm (the translation parameters were similar to Human Experiment 2). Grating flashes happened 84 ms or108 ms after virtual monitor and texture displacement. Note that we reduced the number of flash times here because of the larger number of conditions (5 different spatial frequencies) that needed to be collected. However, our data were consistent with all other experiments in terms of recovery time courses of suppression (e.g. Figs. 1, 3, 4; Figs. S7, S8).

Because the initial displaced position of the virtual monitor (and texture) provided a cue to subjects that grating onset was expected soon, and because such a cue was not present in the one third of trials without image motion, we equalized subject expectations across these conditions by dimming the fixation point to black from the time of image motion onset until 200 ms after flash onset (equal timing was ensured in the one third of trials without image motions, such that the same expectation of grating onset was established by fixation marker dimming). The fixation marker then disappeared, and subjects had to report flash location.

Subjects performed 6 sessions each of this condition, with 576 trials per session (2 subjects performed 7 and 5 sessions each instead of 6).

Finally, we repeated the same experiment but with a black surround around the virtual monitor instead of a coarse or fine texture. Note that a black surround is theoretically equivalent to an infinitely coarse surround. We therefore expected results conceptually similar to those with a coarse surround. Also, in this control experiment, we randomly interleaved all trial types together in the same session (fixation with virtual monitor displacement, real saccade, and fixation with neither virtual monitor displacement nor saccade). This allowed us to further confirm that our results from Human Experiment 3 were not influenced by the separate blocking of real saccade trials and virtual monitor displacement trials.

Retina electrophysiology data analysis and statistics

Low-density MEA recordings were high-pass filtered at a 500 Hz cutoff frequency using a tenth-order Butterworth filter. We extracted spike waveforms and times using thresholding, and we semi-manually sorted spikes using custom software. For high-density MEA recordings, we performed spike sorting by an offline automatic algorithm (Diggelmann *et al.*, 2018) and assessed the sorted units using UnitBrowser (Idrees *et al.*, 2016). We judged the quality of all units using inter-spike intervals and spike shape variation. Low quality units, such as ones with high inter-spike intervals, missing spikes or contamination, were discarded. All firing rate analyses were based on spike times of individual units.

We first characterized the properties of RGCs. We calculated linear filters in response to full-field Gaussian flicker and binary checkerboard flicker by summing the 500-ms stimulus history before each spike. The linear filters allowed determining cell polarity. Specifically, the amplitude of the first peak of the filter was determined. If the peak was positively deflected, the cell was categorized as an ON cell; if negatively deflected, the cell was an OFF cell. ON cells were later always analyzed with respect to their responses to bright probe flashes in the main experiment, and OFF cells were analyzed against dark probe flashes. We determined the spatial receptive fields of RGCs by calculating the linear filters for each region (checker) defined by the binary checkerboard flickering stimulus. The modulation strength of each linear filter, measured as the s.d. along the 500 ms temporal kernel, is an estimate for how strongly that region drives ganglion cell responses. We fitted the resulting 2D-map of s.d. values with a two dimensional Gaussian and took the 2-σ ellipse (long axis) as the receptive field diameter. For all other figures and analyses, we converted spike times to estimates of firing rate by convolving these times with a Gaussian of σ=10 ms standard deviation and amplitude $0.25\ \sigma^{-1}e^{1/2}$.

For each RGC, we used responses to full-field contrast steps to calculate an ON-OFF index, a transiency index, and a response latency index. These indices were used to characterize the properties of RGCs (Fig. S6) that we included in our analyses. The ON-OFF index was calculated by dividing the difference between ON and OFF step peak response by their sum. The resulting index values ranged between -1 (OFF) and +1 (ON) and were then scaled to span between 0 (OFF) and +1 (ON). The transiency index was defined as the ratio of the response area within the first 400 ms and the total response area spanning 2,000 ms. The resulting index had a value of 1 for pure transient cells. Response latency was calculated as the time from stimulus onset to 90% of peak response. This value was normalized to the maximum response latency in our dataset to create the response latency index.

To quantify retinal "saccadic suppression", we first determined a "baseline response", defined as the response to a probe flash approximately 2 s after texture displacement onset (delay between 1,967 to 2,100 ms, depending on the specific flash times used in a specific experiment). This baseline response was compared to responses of the same cell to the same flash when it occurred at an earlier time (i.e. closer in time to the "saccade"). Usually, the saccade-like texture displacements themselves caused significant neural responses even without flashes ("saccade-response", e.g. Fig. 2B), and the responses to the flashes were superimposed on these "saccade-responses" (Fig. 2C). We therefore first isolated the component of the responses caused by the flashes by subtracting the "saccade-responses" from the composite responses.

To estimate the response to "saccades" alone (i.e. without any flashes), we calculated spike rate from before "saccade" onset up until the next "saccade" onset for conditions in which no flash was presented, or until just before the flash onset for conditions in which a "post-saccade" flash was presented. This was done for each of the 39 successive "saccades" in a given trial.

We then computed a neural modulation index, ranging from -1 (complete suppression of flash-induced responses) to +1 ("complete enhancement" of flash-induced responses, i.e. there is only a flash response after saccades, but not to a flash in isolation); a modulation index of 0 meant no change in flash-induced response relative to the "baseline" response. The modulation index of a RGC for a given flash delay, d, relative to a "saccade" onset was calculated as $(r_d - r_b)/(r_d + r_b)$ where r_d is the peak firing rate for the flash-component of the response (see above for how we isolated this from the composite "saccade"+flash response) and r_b is the peak firing rate for the baseline flash response (i.e. the same flash but occurring ~2 s away from any "saccade"; see above). In all cases, peak firing rate was estimated after averaging responses from all repetitions of a given condition (delay d or baseline) for a given RGC. For ON cells, the modulation index was based only on responses to bright flashes, and for OFF cells, it was based on responses to dark flashes. For some analyses, we also calculated modulation indices of neurons for each of the 39 individual "saccades" using the same procedure.

In some cells and trials, individual "saccades" from the sequence of 39 were discarded. This happened when the baseline response peak was less than 60% of the median baseline response peak across the 39 "saccades" of a given trial. We did this to ensure that our modulation

indices were not marred by a denominator approaching zero (e.g. if both flash and baseline responses were weak). Our main results (e.g. Fig. 2) were highly robust to such scenarios.

Finally, to perform statistics, we applied tests at either the individual cell level or at the level of the population. At the individual cell level, we determined whether a given RGC's modulation index for a probe flash presented at a given delay was significantly different from 0 (i.e. "Is the response of this cell modulated by the 'saccade'?"). For this, we performed a one-tailed sign test of the null hypothesis that the 39 individual modulation indices came from a distribution with zero median against the alternative hypothesis that the median was below (for negative modulation index) or above (for positive modulation index) zero. The modulation index was considered significant (i.e., the flash response was modulated by the "saccade") at $p<0.05$ if the test had a power ($1-\beta$) of at least 0.8. At the population level, we determined whether the retinal output as a whole was modulated by "saccades". For this, we performed a two tailed Wilcoxon signed rank test of the null hypothesis that the median of the distribution of modulation indices did not differ from 0. Lastly, we tested whether the modulation index of the population, was significantly different across textures. For this, we performed a two tailed Wilcoxon signed rank test of the null hypothesis that the median of the distribution of modulation indices did not differ across textures. Since our modulation index was based on responses to the brief probe flashes, it could only be computed for cells that did respond to these flash stimuli (mouse: N = 688 of 1,423 recorded cells; pig: N = 228 of 394). Only these cells, showing a measurable baseline flash response, were included in our analyses for retinal "saccadic suppression" (Fig. 2E, Fig. S5).

Human psychophysics data analysis and statistics

We analyzed eye movements in all trials. We detected saccades using established methods (Chen and Hafed, 2013), and we manually inspected all trials to correct for mis-detections. In experiments requiring a saccade (e.g. Fig. 1), we excluded from analysis any trials with premature (before saccade instruction) or late (>500 ms reaction time) saccades. We also rejected all trials in which saccades landed >0.5 deg from the saccade target. In experiments requiring fixation, we excluded from analysis any trials in which a saccade or microsaccade happened anywhere in the interval from 200 ms before to 50 ms after any flash or grating onset.

For experiments with saccades (e.g. Fig. 1), we obtained time courses of perception by calculating, for each trial, the time of flash or grating onset from saccade onset. We then binned these times into 50 ms bins that were moved in 5 ms bin-steps relative to saccade

onset. Within each bin, we calculated the proportion of correct trials, and we obtained full time courses of this perceptual measure. We obtained time course curves for each subject individually, and we then averaged the curves for the individual subjects in summary figures. All of our analyses were robust at the individual subject level as well (e.g. Fig. S2).

For experiments with simulated "saccades" (i.e. saccade-like texture displacements), there were discrete flash or grating times relative to "simulated saccade" onset, so no temporal binning was needed. At each flash or grating time, we simply calculated the proportion of correct trials.

When we fitted performance to psychometric curves (e.g. Fig. S3A, B), we used *the psignifit 4 toolbox* (Schütt *et al.*, 2016), and we used an underlying beta-binomial model.

For some analyses of Human Experiment 3 and its control version, we calculated a "suppression ratio". This was obtained as follows. For a given spatial frequency grating, we calculated the fraction of correct trials within a given time window (from either simulated or real saccade onset) divided by the fraction of correct trials for the same spatial frequency when there was neither a saccade nor a virtual monitor and texture displacement (i.e. baseline perception of a given spatial frequency). This ratio therefore revealed the effect of suppression independently from the underlying visibility of any given spatial frequency (Chen and Hafed, 2017).

All error bars that we show denote s.e.m. across individual subjects, except when we showed individual subject analyses and control analyses. For individual subject performance, error bars denote s.e.m. across trials; for control analyses, error bars denote 95% confidence intervals (e.g. Fig. S3A, B) or s.d. (e.g. Fig. S3D, F). All error bar definitions are presented in all figures and/or legends.

For real saccades with time courses of performance relative to saccade onset, we were interested in comparing the time courses of perception across background textures (i.e. coarse versus fine). To statistically validate if the time courses for perceptual localization for the different background textures differed significantly from each other, we used a random permutation test with correction for time clusters of adjoining significant p-values (Maris and Oostenveld, 2007; Bellet, Chen and Hafed, 2017). First, for each time bin, we calculated a test statistic comparing performance for coarse versus fine background textures. This test statistic was the difference between the proportion of correct responses for the different textures. Then, we performed a random permutation with 1,000 repetitions for each time bin; that is, we collected all trials of both conditions, within a given time bin, into a single large set, and

we randomly assigned measurements as coming from either coarse or fine textures, while at the same time maintaining the relative numbers of observations per time bin for each texture condition. From this resampled data, we calculated the test statistic again, and we repeated this procedure 1,000 times. Second, we checked, for each time bin, whether our original test statistic was bigger than 95% of the resampled test statistics (i.e. significant), and we counted the number of adjoining time bins that were significant at this level (i.e. clusters of time bins in which there was a difference between coarse and fine textures). We then repeated this for all 1,000 resampled test statistics. The p-value for our original clusters was then calculated as the number of resampled clusters that were bigger or the same size as the original clusters, divided by the total number of repetitions (1,000). This procedure was described in detail in (Bellet, Chen and Hafed, 2017). We followed a conservative approach, paying no attention to which bins in the resampled data formed a cluster of time bins. As discussed elsewhere (Bellet, Chen and Hafed, 2017), our statistical analysis constituted a highly conservative approach to establishing significance of differences between time courses for coarse and fine textures. In Human Experiment 3, we used the same approach to compare time courses of suppression ratio for coarse and fine surround contexts with real saccades.

For Human Experiment 2, we had discrete flash times relative to texture displacement onset. Here, the comparison between coarse and fine textures was tested with a Bonferroni-corrected χ^2 test at corresponding flash times. To compare between real and simulated saccades in Human Experiments 1 and 2, we also ran a Bonferroni-corrected χ^2 test. We only considered time bins in the real saccade data that corresponded to the discrete flash times in the simulated saccade data. A Bonferroni correction was necessary because we tested the same data sets on multiple time bins with the same hypothesis (that there is a difference in time courses).

In Human Experiment 3, we also compared suppression ratios for real and simulated saccades for a given texture surround. We again used a Bonferroni-corrected χ^2 test. This was justified because within a given surround, baseline data were the same for real and simulated saccades. Therefore, the relationship between the proportion of correct localizations and suppression ratio was identical. In contrast, testing suppression ratios between fine and coarse surrounds in the same experiment with a χ^2 test was not applicable because baseline values differed. Therefore, we used instead a random permutation test with 5,000 repetitions. To compare the different spatial frequency Gabor gratings in one bin or time stamp, we used the Kruskal-Wallis test.